Journal of Natural Gas Science and Engineering 35 (2016) 1180–1199

Contents lists available at ScienceDirect

Journal of Natural Gas Science and Engineering

journal homepage: www.elsevier.com/locate/jngse

# Enabling utility-scale electrical energy storage by a power-to-gas energy hub and underground storage of hydrogen and natural gas

Dan D. Peng [a], Michael Fowler [a], Ali Elkamel [a, b], Ali Almansoori [b, *], Sean B. Walker [a]

[a] Department of Chemical Engineering, University of Waterloo, Waterloo, Ontario, N2L 3G1, Canada
[b] Department of Chemical Engineering, The Petroleum Institute, P.O. Box 2533, Abu Dhabi, United Arab Emirates

ARTICLE INFO

*Article history:*
Received 18 April 2016
Received in revised form
14 August 2016
Accepted 14 September 2016
Available online 15 September 2016

*Keywords:*
Hydrogen
Natural gas
Underground storage
Emissions
Energy systems
Process modeling
Process simulation

ABSTRACT

With the increased use of renewable energy, energy storage technologies are becoming increasingly important. One such technology is Power-to-Gas, which can provide seasonal energy storage by utilizing both the electrical and natural gas infrastructures through injecting hydrogen into existing gas infrastructure to create Underground Storage of Hydrogen and Natural Gas (UHNG). The hydrogen is recovered from the mixture as needed for industry or transportation applications, converted to electricity to meet power demand, or kept as a mixture of hydrogen-enriched natural gas to serve gas demand. Large scale energy storage is desirable to energy generation operators for its ability to manage excess base load energy, integrate renewable energy into the grid and provide long term energy storage. The authors investigate the financial and environmental performance of specific scenarios of UHNG produced by Power-to-Gas through scenario-based simulations in a MATLAB/Simulink for comparative purposes. The simulated scenarios include the injection of hydrogen for long term storage, load shifting, renewable energy integration and supplying a large hydrogen demand. All of these scenarios are compared to a base case which simulates the operations of a conventional underground gas storage facility. The analysis illustrates that existing natural gas storage practices are driven by variations in the demand for natural gas. The most desirable pathway for energy recovery and revenue in this analysis occurs when hydrogen is injected into the reservoir along with natural gas and is distributed to off-site users.



## 1. Introduction

Currently, there is a collective effort to decrease global carbon emissions by including more renewable power generation into the supply mix. In Ontario, for example, renewable generation is expected to reach 10,700 MW by 2015 (Ontario Ministry of Energy (2012)). With this increase comes a demand for energy storage to mediate between intermittent supplies of renewable energy that must be dispatched to meet varying demands from the electrical grid (Baxter, 2006). Although curtailment is possible during periods of surplus, fixed Feed-in-Tariff (FIT) contracts with renewable energy generators make it economically unfavorable. This loss in supply flexibility will increase as renewable energy generators gain higher penetration in the grid.

Energy storage through Underground Hydrogen and Natural Gas (UHNG) is a proposed energy storage technology. To use UHNG, electricity is converted to hydrogen, blended with natural gas and stored underground or sent to end users through the gas distribution system. After storage, the hydrogen may be retrieved and routed to either Power-to-Gas, Power-to-Power or Power-to-Hydrogen. In Power-to-Gas the hydrogen-enriched natural gas (HENG) is delivered to end-users for existing applications including heat, electricity generation or industrial applications; in Power-to-Power the gas mixture is sent to generate electricity; and in Power-to-Hydrogen the gas mixture is separated into its components and consumed by end-users. This paper is an analysis of Power-to-Gas as an energy storage option. Previous energy storage reviews provide comparisons between energy storage options but do not examine Power-to-Gas (Sandia, 2013; EPRI, 2010).

UHNG is a utility-scale energy storage technology which uses electrolyzers to generate and inject hydrogen into the natural gas system. The use of the pre-existing natural gas infrastructure provides technological and economic advantages.

Underground storage has previously been suggested for $CO_2$ sequestration (Bachu and Dusseault, 2005; Dusseault et al., 2004). Unlike carbon capture, underground storage of $H_2$ makes it possible

* Corresponding author.
*E-mail address:* aalmansoori@pi.ac.ae (A. Almansoori).

http://dx.doi.org/10.1016/j.jngse.2016.09.045
1875-5100/

to meet electrical demands while keeping a constant fraction of hydrogen in the natural gas (Schouten et al., 2004). Due to the volume of the natural gas infrastructure, the hydrogen concentration easily stays below 5% by volume, avoiding possible embrittlement concerns (Altfield and Pinchbeck, 2013). The use of hydrogen-natural gas mixtures can affect the performance of natural gas furnaces, engines and turbines. The $H_2$ concentration can be changed by varying production or the rate of underground storage. However, due to the relative abundance of natural gas in comparison to hydrogen capacity, the effect of a higher or lower $H_2$ concentration on the UHNG hub operation is not investigated. The size of the natural gas grid can also be useful during the transition of cars from fossil fuels to hydrogen (Venter and Pucher, 1997; Schouten et al., 2006). Sarnia, Ontario is an ideal area for UHNG projects, due to the presence of natural gas reservoirs (Venter and Pucher, 1997). The North Sea Fields in the United Kingdom, are also endowed with underground caverns which are suitable for storing hydrogen (Stone et al., 2009). The underground storage of hydrogen is typically carried out in depleted natural gas caverns or salt domes, and where large industrial consumers are connected directly to transmission lines (Melaina et al., 2013). The costs of UHNG are low and come from the costs of the reservoir, injection wells, injection equipment, electricity and maintenance (National Energy Technology Laboratory, 2010; Crotogino et al., 2010; European Union, 2015; Bunger, 2014).

Combining Power-to-Gas and underground storage gives the electrical utility both the flexibility to maintain the grid through ancillary services while providing bulk energy storage. The bulk energy storage allows the seasonally-adjusted storage of significant amounts of power and the provision of $CO_2$-neutral fuels, when renewable energy is used (Germany Trade and Invest, 2012; Bajohr et al., 2011). A drawback of underground storage is its geographic specificity (Mannan et al., 2014).

Traditionally, electricity is generated in centralized locations, and transmitted through great distances to reach customers. In Ontario, nuclear power has provided the majority of the grid's capacity and base load. Compared to other generators, nuclear plants require long lead times to change their power output and, thus, tend to operate at a stable power output. During off-peak hours, Ontario's electricity production from base load facilities is often greater than the provincial demand for power. This excess electricity is exported at a low, occasionally negative, price to neighboring jurisdictions (IESO, 2013).

## 2. Methods

### 2.1. Model overview

In order to study the behavior of UHNG in various scenarios, a series of equations used to form a system model with hourly resolution is built using MatLAB-Simulink. Once the physical behavior of an energy hub employing UHNG is determined for a scenario and a given set of exogenous conditions, the corresponding financial and environmental performance of the system are determined. The components of the energy hub illustrated in Fig. 1 are, wind turbines, electrolyzers, a storage reservoir, a Combined-Cycle Gas Turbine (CCGT) plant and a Pressure Swing Adsorber (PSA) separator. The PSA is chosen for its optimum performance in separating hydrogen and natural gas. The behavior of each component is dependent on fixed technological constraints, as well as conditions and process variables. The exogenous conditions, unless specified, come from historical Ontario electricity market conditions starting in 2009 and ending in 2012 (IESO, 2013). The hydrogen demand may include hydrogen refueling or industrial purposes like petroleum refining and ammonium production. For the Power-to-Gas system, the electrical grid is both a source and a sink of electricity, as the energy hub may both generate and consume electricity. The hydrogen and natural gas in the underground reservoirs is supplied by high pressure transmission pipelines. The mixture withdrawn from storage is not sent back to the natural gas grid: it is assumed that the gas exiting the energy hub, in the form of a natural gas/hydrogen mixture called hydrogen-enriched natural gas (HENG), is distributed directly to consumers within the hub.

Unlike electricity or HENG, the demand for hydrogen does not have dedicated transport infrastructure. Therefore, hydrogen delivery is not continuous as delivery is only possible at discrete points in time for fixed amounts. As scenarios are examined, and not an optimization, variables are provided with estimated preliminary values so that the model is fully specified. The process variables define the configuration, capacity and operation of the energy hub. The colored diamonds D1 through D6, shown in Fig. 1, are decision points where process variables must be specified. Most of the decision points are continuous; however, some have discrete elements. The decision variables are defined as follows:

- D1: energy can be injected into the reservoir, gas can be removed from the reservoir, or the reservoir can be shut-in;
- D2, the amount of power to operate the electrolyzer is chosen;
- D3, the $H_2$ is directed to users or storage;
- D4, the blend of HENG can be manipulated, and;
- D5, amounts of HENG withdrawn or sent to other pathways are calculated;
- D6, the destination of the natural gas-rich stream from the separator is decided.

All of the dynamic behaviors from the physical model are available as an hourly time series. Thus, the corresponding financial and environmental performance is also a time series.

### 2.2. Physical model

The storage reservoir is the most important component of the hub because it is the only component where gas accumulation occurs. Underground storage reservoirs fall into two categories: porous media storage, including aquifers and depleted gas fields, and caverns. Regardless of the type of reservoir, capacity and containment, which depend on pressure, are the key considerations for storing hydrogen (Foh et al., 1979). For a porous reservoir with a known capacity, the capacity is expressed in terms of the standard volume of natural gas at maximum reservoir pressure (Ikoku, 1980). The standard volume of the reservoir is related to the maximum reservoir pores volume through the use of the gas formation volume factor $B_g$.

$$V_{\max} = B_g V_{\max,s} \tag{1}$$

$$B_g = \frac{p_s T_{res} z_{res}}{p_{res} T_s z_s} \tag{2}$$

where $V_{max}$ represents the maximum reservoir pore volume, $V_{max,s}$ is the maximum reservoir capacity for natural gas at standard volume, $p_s$ is the standard pressure, $p_{res,max}$ is the maximum reservoir pressure, $T_s$ and $T_{res}$ are the standard and reservoir temperature, respectively, and $z_s$ and $z_{res,max}$ are the standard and maximum reservoir compressibility factors, respectively.

Once $V_{max,s}$ is known, the actual reservoir pore volume $V_{max}$ is determined for subsequent inventory calculations.

The reservoir inventory changes with the flow of gas in and out of the reservoir. Assuming there is no water influx into the reservoir, and negligible losses from the reservoir during storage, the

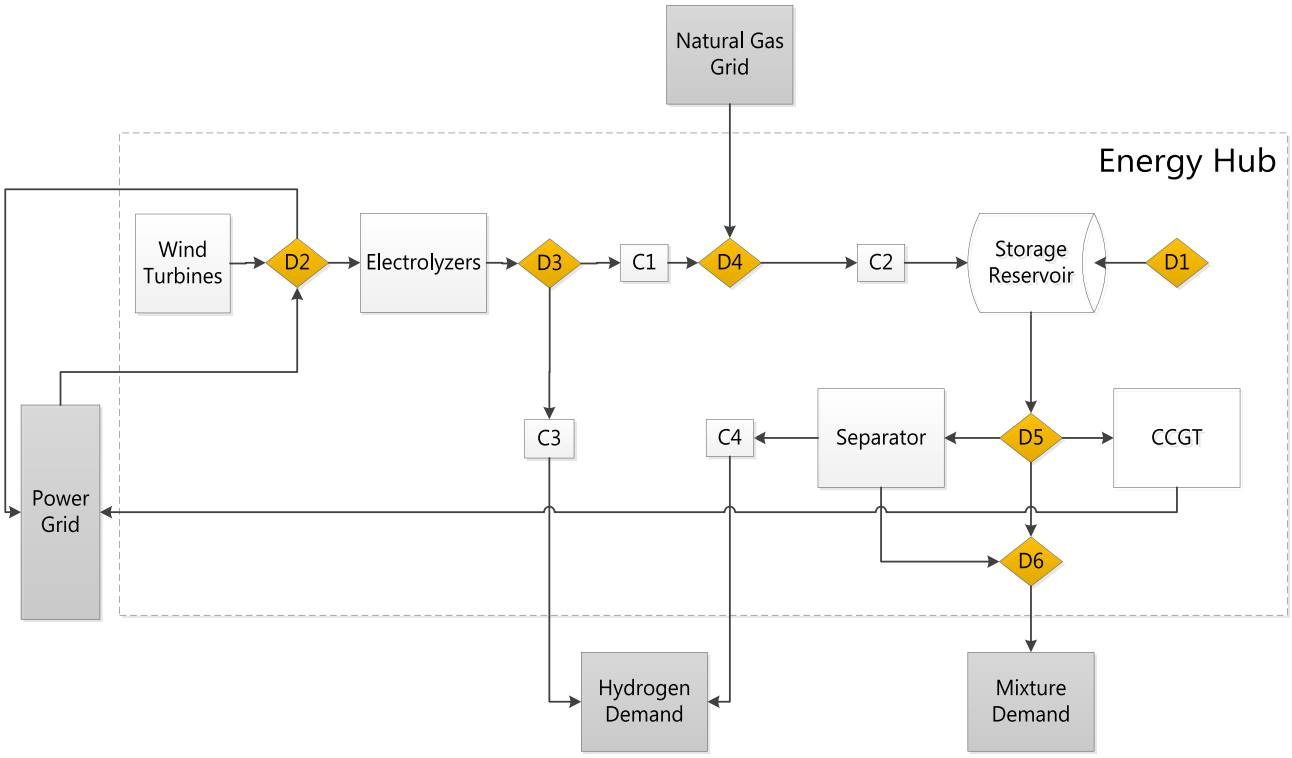


**Fig. 1.** Detailed view of the proposed energy hub.

simplest material balance is where time is treated as discrete steps.

$$n_{tot} = n_{tot,0} + (\dot{n}_{in} - \dot{n}_{out})\Delta t \tag{3}$$

where $n_{tot}$ and $n_{tot,0}$ give the total amount of gas in place at the end and beginning of the time step, respectively and $\dot{n}_{in}$ and $\dot{n}_{out}$ give the injection rate and production rate of gas during the time step, respectively.

In this model, injection and withdrawal cannot take place at the same time, thus, (3) simplifies to (4):

$$n_{tot} = n_{tot,0} + (\dot{n}_{s,act})\Delta t \tag{4}$$

Here, $\dot{n}_{s,act}$ is positive when gas is injected and negative when gas is withdrawn. While injecting gas from the reservoir, the average reservoir pressure, and the gas inventory are subjected to two constraints. First, the average reservoir pressure, $\overline{p}_{res}$ cannot exceed the maximum allowable reservoir pressure, $p_{res,max}$, as shown in Eq. (5).

$$\overline{p}_{res} \leq p_{res,\max} \tag{5}$$

Secondly, as shown in Eq. (6), the average reservoir pressure ($\overline{p}_{res}$) cannot fall below the minimum allowable reservoir pressure $p_{res,min}$.

$$\overline{p}_{res} \geq p_{res,\min} \tag{6}$$

In the reservoir, the driving force for gas injection and production is the pressure difference between the reservoir and the surface (Clarke, 2012). Therefore, the flow of gas that can be injected or delivered is a function of the reservoir and wellhead pressures.

Modern wind turbines utilize a horizontal-axis design. The empirical relationship between the power output of a turbine and the wind speed is related by Eq. (7).

$$P_{W,i} = f(u_{80}) \tag{7}$$

where $u_{80}$ is the wind speed 80 m above the ground and $P_{W,i}$ represents the rated capacity of the turbine unit.

The V90 2.0 MW is a pitch-regulated turbine that is suitable for sites with medium to low wind speeds. For wind speeds below 14 m/s, the power curve is a function of wind speed. For wind speed of 14–25 m/s, the V90 generates power at its rated capacity, 2 MW. At wind speeds below 4 m/s, the cut-in speed, or higher than 25 m/s, the cut-out speed, the wind turbine is not operated and the power output is zero (Vestas, 2015). The hourly wind speed for the region of Sarnia at a height of 10 m, where the reservoir is located, is known for the simulation period. The wind speed is adjusted to a height of 80 m, as per the correlation in Eq. (8)

$$u_{80} = u_{10}\left(\frac{80m}{10m}\right)^{\alpha} \tag{8}$$

where $u_{10}$ is the wind speed at 10 m above the ground and $\alpha$ is the Hellman exponent.

The rated power output of the wind farm is the total of the rated power for each unit. For identical wind turbines, Eq. (9) is used.

$$P_{W,rated} = N_T P_{W,i,rated} \tag{9}$$

A the rated power of each unit is fixed, the number of turbines in place $N_T$, changes to alter the total rated power. As with rated power, the power generated on a wind farm is the sum of the generation from each turbine.

$$P_W = N_T P_{W,i} \tag{10}$$

The energy requirement of an electrolyzer varies with hydrogen production capacity and efficiency. Electrolyzer stacks use about 90% of the total energy requirement (Brown, 1997). The stack

energy requirement changes with efficiency. For example, at 100% efficiency, the work required to produce hydrogen is the higher heating value (HHV) of hydrogen.

$$P_{E,i} = \dot{n}_{E,H_2,i} E_E \tag{11}$$

$$E_E = E_{E,s} + E_{E,a} = E_{E,s}/0.90 \tag{12}$$

$$E_{E,s} = \frac{E_{HHV}}{\eta_{E,s}} \tag{13}$$

$$\dot{n}_{E,H_2,i} = \frac{0.90\eta_{E,s} P_{E,i}}{E_{HHV}} \tag{14}$$

The efficiency of the electrolyzer is a function of the cell operating voltage and the current density which is a function of hydrogen production. Thus, the energy requirement of an electrolyzer can be re-written as a function of hydrogen production alone. For power generation, the efficiency of the CCGT is dependent on the gas and steam turbine efficiencies. The two thermal cycles are connected through the heat recovery steam generator, where the exhaust from the gas turbine exchanges heat with the condensate of the steam cycle, forming more steam. The overall efficiency is a function of the steam turbine and gas turbine heat inputs and power outputs, given in Eq. (15).

$$\eta_{CC} = \frac{\dot{W}_{GT} + \dot{W}_{ST}}{\dot{H}_{GT} + \dot{H}_{ST}} \tag{15}$$

The efficiency of the gas turbine cycle is pre-determined for a fuel hydrogen concentration from 0 to 20% and relative fuel flow rate between 50 and 100%. Once the part-load gas turbine cycle efficiency is known, it is used to find the part-load combined cycle efficiency. The efficiency of the gas turbine cycle is dependent on the heat rate, which also influences the efficiency of the overall combined cycle due to its effect on the steam turbine cycle efficiency. In this model the CCGT is modeled with one overall efficiency. The PSA, is characterized by the percentage of desired product present in the mixture that is recovered after separation. In future, other processes such as electrochemical separation may be developed to improve this separation step. For this energy hub, the recovery of hydrogen is calculated by Eqs. (16) and (17):

$$\eta_{sep} = \frac{\dot{n}_{H_2}}{\dot{n}_{H_2,feed}} = \frac{c_{H_2,product}\dot{n}_{product}}{\dot{n}_{feed}c_{H_2,feed}} \tag{16}$$

$$\dot{n}_{H_2,sep} = \eta_{sep}\dot{n}_{Feed}c_{H_2,Feed} \tag{17}$$

where $\eta_{sep}$ is the separation recovery efficiency of the PSA, $\dot{n}_{H2}$ is the amount of hydrogen recovered, $\dot{n}_{H2,\ feed}$ is the amount of hydrogen fed to the system, $\dot{n}_{feed}$ is the total amount of feed sent to the electrolyzer and $c_{H2,\ feed}$ is the concentration of hydrogen in the feed.

The power required by the compressor is a function of the gas flow and the inlet and outlet conditions. The work and effluent conditions are estimated based on the inlet conditions and discharge pressure. For simplicity, isentropic conditions without friction are assumed. As the compression pressure ranges from atmospheric pressure to hundreds of bar, deviation from the ideal gas behavior is accounted with the compressibility factor, z, which impacts reservoir inventory calculations, as outlined in Equation (18) and (19) (Dranchuk et al., 1973; Elsharkawy and Elkamel, 2001; Fatoorehchi et al., 2014, 2014a). For example, compressing gas from 1 to 100s of bars would require multi-stage compressors with intercoolers. In this simulation, a simple assumption of an overall efficiency of 60% was used as a proxy for such a system.

$$P_{comp} = \dot{n}_{comp}\frac{W_{comp,th}}{\eta_{comp}} \tag{18}$$

$$W_{comp,th} = RT_{in}\frac{k_{mix}}{k_{mix}-1}\left[\left(\frac{p_{out}}{p_{in}}\right)^{\bar{z}(k_{mix}-1)/k_{mix}} - 1\right] \tag{19}$$

where $W_{comp,th}$ gives the isentropic work done by the compressor, $P_{comp}$ is the actual power required by the compressor, $\dot{n}_{comp}$ is the compression gas flow rate, and $\eta_{comp}$ is the compressor isentropic efficiency. $k_{mix}$ is the heat capacity ratio of the compressed gas.

### 2.3. Financial model

Once the revenues from all four sales streams, wind power to grid, hydrogen to end users, CCGT to grid, and HENG to end users, are calculated, the total sales are obtained by summing these values over the period of interest. In this case, for annual financial evaluations, the sales are summed over each of the years simulated, as shown in Eq. (24) where all of the sales streams are added up for the total number of years of the project.

$$S_{annual} = \sum_{1}^{t}\left[S_{wtG}(t) + S_{H_2}(t) + S_{CCTGtG}(t) + S_{mix}(t)\right] \tag{24}$$

The annual variable costs consist of two components, the purchase of natural gas and the purchase of electricity. The total cost of purchases is calculated by multiplying each flow rate by the corresponding market price as in Eqs. (25) and (26).

$$C_{Gts}(t) = P_{Gts}(t)HOEP(t) \tag{25}$$

$$C_{NGts}(t) = \dot{n}_{NG,in}(t)E_{NG}C_{NG}(t) \tag{26}$$

where $C_{Gts}$ is the cost of power, $C_{NGts}$ is the cost of natural gas, and Hourly Ontario Energy Price (HOEP(t)) is the wholesale price of electricity at a time t (IESO, 2015).

Because wind turbines are an integral part of the energy hub, wind power supplied to the electrolyzer does not constitute a purchase, for money has not been transferred between two entities: the operators of the wind turbines are also the operators of the energy hub. The total cost of all energy purchases over the period of interest is summed as follows:

$$C_{annual} = \sum_{1}^{t}\left[C_{Gts}(t) + C_{NGts}(t)\right] \tag{27}$$

The total purchase cost for starting material, incurred at the time of purchase, can be separated into two components: the cost of material incurred and the inventoried purchase cost, which is the portion of the purchase cost which is attributable to inventory accrued over the year.

$$C_{annual} = I + C_{incurred} \tag{28}$$

where $C_{annual}$ and $C_{incurred}$ are the annual purchase of energy and the incurred cost, respectively and I is the inventoried cost of purchase.

$I$ is equivalent to the change in inventory value over the course of a year and is also the portion of the annual expenses that can be deducted from the annual income statement and can be positive or negative.

At the beginning of the simulation, the value of gas in storage $C_{res,tot}(t_0)$ is estimated using the initial physical inventory $n_{total}$ and the estimated unit cost of the gas stored as given by the following equation. At the beginning of the simulation, the gas is pure natural gas and thus the cost of the gas is the natural gas price.

$$C_{res,tot}(t_0) = C_{mix,unit,0} n_{tot,0} \tag{34}$$

Then, the value of inventory and the unit cost of stored gas are updated hourly according to Eqs. (35) and (36).

$$C_{res,tot}(t) = \begin{cases} C_{res,tot}(t-1) + \dot{n}_{s,act}(t) C_{mix,unit}(t-1), & \text{if } \dot{n}_{s,act}(t) < 0 \\ C_{res,tot}(t-1) + C_{NGts}(t) + C_{Gts}(t) \dfrac{\dot{n}_{H_2,S}(t)}{\dot{n}_{H_2,E}(t)}, & \text{if } \dot{n}_{s,act}(t) \geq 0 \end{cases} \tag{35}$$

$$C_{mix,unit}(t) = \frac{C_{res,tot}(t)}{n_{tot}(t)} \tag{36}$$

where $\dot{n}_{s,act}$ is the flowrate through the reservoir, $\dot{n}_{H_2,S}$ is the amount of stored $H_2$ and $\dot{n}_{H_2,E}$ is the amount of electrolytic $H_2$ produced. The capital cost of the energy hub, $C_{inv,tot}$, is based on the rated input or output capacity of its constituents. The purchase costs of the turbines $C_{W,inv}$, electrolyzers $C_{E,inv}$, compressors $C_{comp,inv}$, the separator unit $C_{sep,inv}$ and the CCGT $C_{CCGT,inv}$ make up most of the capital cost.

$$C_{inv,tot} = C_{W,inv} + C_{E,inv} + C_{sep,inv} + C_{CCGT,inv} + C_{comp,inv} \tag{37}$$

With the total capital cost value determined, the capital recovery factor is used to make the total capital investment, a one-time cash flow at the beginning of the project, into a series of constant annuities over the course of project life. The capital cost of wind projects in Canada is given as a function of project rated capacity as given by the following Eq. (38) (IREA, 2012). This method will generate an approximate figure that can be used to determine the relative economic performance of the project.

$$C_{W,inv} = \$2,000,000 \frac{CEPCI_{2008}}{CEPCI_{2006}} P_{W,rated} \tag{38}$$

$CEPCI_{2008}$ and $CEPCI_{2006}$ are the chemical engineering plant cost index for 2008 and 2006, respectively.

It is known that for hydrogen production scale ranging from 0.05 kmol/h to 50 kmol/h, only one unit of electrolyzer is needed, and economies of scale are possible.

$$C_{E,inv} = 224,490 \left(2\dot{n}_{E,H_2,rated}\right)^{0.6156} \quad 0.05 \leq \dot{n}_{E,H_2,Rated} \leq 50 \tag{39}$$

The 2.7 kmol/h, HySTAT-60 from Hydrogenics electrolyzer, has been chosen for this model. The capital cost required for an individual unit is thus given by Eq. (40) (IREA, 2012).

$$C_{E,inv,i} = \$224,490 \left(2\dot{n}_{E,H_2,rated,i}\right)^{0.6156} \tag{40}$$

The total capital cost for electrolyzers depend on the number procured ($N_E$) as given by Eq. (41).

$$C_{E,inv,0} = N_E C_{E,inv,i} \tag{41}$$

The main capital investment for a PSA system consists of the purchase of adsorption beds $C_{sep,ads}$ and PSA vessel $C_{sep,col}$. Compressors are not required for feed pressurization, because reservoir gas is available at pressures above 20 bar, the stated operating pressure of the adsorption columns. However, the residue gas would need to be compressed. There are a number of approaches to determining the cost of a PSA system, such as that of Chung et al. (1998).

$$C_{sep,inv} = C_{sep,ads} + C_{sep,col} \tag{42}$$

For the expected capacity range below 200 MW, the investment cost of CCGT power plants is estimated to be $650/kW, in 2006 dollars (IREA, 2012). This cost is converted to 2008 dollars by Eq. (43).

$$C_{CCGT,inv} = \$650,000 \left(\frac{CEPCI_{2008}}{CEPCI_{2006}}\right) \dot{W}_{CC,rated} \tag{43}$$

The capital investment required by the compression unit is given by Eq. (44).

$$C_{comp,inv} = P_{comp,rated} C_{comp} \tag{44}$$

The operation and maintenance cost for the hub has both fixed and variable costs. The fixed maintenance cost is assumed to be a percentage ($R_{OM}$) of the annual capital cost, as shown in Eq. (45).

$$C_{OM,fixed} = R_{OM} C_{inv,annual} \tag{45}$$

The variable operating cost is due to the consumption of energy by the reciprocating compressors used on-site. It is assumed that the compressors used at the hub are powered by natural gas engines and the energy consumption is converted to natural gas consumption ($NG_{comp,NG}$), using conversion factors.

$$NG_{comp,NG} = P_{comp} \frac{GPR}{E_{NG}} \tag{46}$$

where $P_{comp}$ is the power requirement for the compressor, GPR is the gas energy per unit of electrical energy, $E_{NG}$ is the energy content of the natural gas. The cost of energy consumed by the compressors is then calculated in Equation (47):

$$C_{comp,E}(t) = P_{comp,NG}(t) C_{NG}(t) \tag{47}$$

The annual operating and maintenance is the sum of the fixed cost and the annual variable costs shown in the equations above and is given by the following equation.

$$C_{OM,annual} = C_{OM,fixed} + \sum_{1}^{t} C_{comp,E}(t) \tag{48}$$

### 2.4. Emission model

The $CO_2$ emissions impact of the energy hub equals the

emissions incurred by the energy hub, $m_{CO_2,incurred}$, minus those mitigated by the hub $m_{CO_2,mitigated}$. The net emissions impact is thus given by Equation (49).

$$m_{CO_2,net} = m_{CO_2,incurred} - m_{CO_2,mitigated} \quad (49)$$

The $CO_2$ emissions associated with the operation of the energy hub are attributed to the use of natural gas driven compressors, grid-generated electricity, electricity generated from turbines, CCGT for energy recovery, and the off-site use of HENG. The total value of $CO_2$ emissions is estimated by t following Equation (50).

$$m_{CO_2,incurred} = m_{CO_2,comp} + m_{CO_2,G} + m_{CO_2,W} + m_{CO_2,CCGT} + m_{CO_2,mix} \quad (50)$$

When the hydrogen is not stored in UHNG, pure natural gas is used to generate electricity or is distributed to end-users. When UHNG is used on-site at the hub and distributed off-site, the mitigation of greenhouse gas emissions is possible. Carbon emission mitigation is accomplished by the use of hydrogen from electrolysis instead of from steam methane reforming (SMR), the industry norm for hydrogen production, and from the use of HENG which burns cleaner than natural gas. The emissions from SMR are displaced when the system provides hydrogen for an industrial application; emissions for fuel are displaced when the hydrogen is used for transporation fuel; and, emissions from natural gas are mitigated when the hydrogen is injected into the pipeline.

$$m_{CO_2,mitigated} = m_{CO_2,SMR} + m_{CO_2,fuel} + m_{CO_2,NG} \quad (51)$$

### 2.5. Scenarios generation

Five scenarios are used to examine the impact of hydrogen storage on system performance.

The following scenarios are used:

- Scenario 1 – Base Case – Only Natural Gas (NG) into reservoir
- Scenario 2 – Injection of $H_2$ and NG into reservoir
- Scenario 3 – Injection of $H_2$ and NG into reservoir with Combined Cycle Gas Turbine (CCGT) to recover power as electricity
- Scenario 4 – Injection of $H_2$ and NG into reservoir with CCGT to produce electricity and wind turbines to power the electrolyzer
- Scenario 5 – Injection of only $H_2$ into reservoir for long-term energy storage

The first scenario, or base case, involves the operation of an underground gas storage facility without the production or storage of hydrogen. The driving force in this scenario is the natural gas profile which has lower prices in the summer and higher prices during the winter. In the second scenario, electrolyzers are added as a key component of the hub which brings connectivity to the grid and the demand for hydrogen. The use of the electrolyzers is triggered by a lower electricity price, which indicates a plentiful electricity supply. The hydrogen is either blended with natural gas for storage, or consumed directly, if injection is not possible. As in the first scenario, the injection and withdrawal schedule of the reservoir is based on fluctuations in the market price of natural gas. The third scenario involves the reduction of surplus base load generation. It differs from the previous scenarios in that the on-site CCGT is included in the hub, so that the stored energy can be recovered in the form of electric power. The configuration in the third scenario allows the hub operators to store electricity from and deliver electricity to the grid at the same location. The triggering signal is the trend in the electricity price. Natural gas blended with electrolytic hydrogen (HENG) is stored when there is an oversupply in the electricity market, and it is used to fuel the on-site CCGT power generation when electricity demand is high. In the fourth scenario wind turbines are added to the energy hub described in the third scenario. The wind turbines are within the boundary of the hub, as it is assumed that they have the same properties and operators as the rest of the energy hub. In this scenario, hydrogen is produced and injected into the reservoir, forming HENG, when the demand for wind power is low. The stored energy is released via the on-site CCGT power generation when the demand for wind power is high. The proxy used to indicate demand for wind power is the time-differentiated feed-in tariff price for wind turbine operators because it offers a clearer understanding of when the renewable energy is needed than overall demand. In the fifth scenario it is assumed that energy is mainly used for hydrogen production, and that the storage reservoir is transitioning toward a pure hydrogen storage facility. In this case, only hydrogen is injected to the reservoir. Assuming that natural gas with relatively high percentages of hydrogen is produced from the reservoir, the main pathway for energy recovery is the purification of the produced gas through a PSA separator. The natural gas-rich waste from the separator contains little hydrogen and is subsequently distributed through the natural gas distribution system. Hydrogen is again produced when the market price of electricity is low and it is directly dispatched for use if the time of production coincides with the time of use. Otherwise, pure hydrogen is injected into the reservoir for later retrieval and purification. The hydrogen demand schedule is assumed and fixed at the beginning of the simulation. In this paper, Ontario natural gas and electrical data is used to form the simulation. Furthermore, the work is based on the thesis of the first author (Peng, 2013). The thesis is cited throughout the document and more details are available there.

## 3. Results

In this section, the results of each of the different scenarios are presented so that the impact of the various configuration, scale and logic at decision points can be evaluated. All simulations last for a period of three years, from 2010 to 2012, inclusively. The labels of the time axis in the figures presented in this section and in the next section identify the resolution of each graph displayed: Hour of time (hourly), day of time (averaged by day), or week of time (averaged by week).

### 3.1. First scenario: base case of underground gas storage

In Fig. 2, the dispatch order placed on the reservoir and its injectability or deliverability during the simulation is illustrated. A reservoir mode of 1 indicates an order to inject gas into the reservoir, of −1 to produce gas from the reservoir, and of 0 to shut-in the reservoir. In Fig. 2, it is shown that the dispatch orders to the reservoir alternate semi-regularly with injection and withdrawal periods of unequal duration. Due to the model logic specified at decision points D4 and D5, the actual flow of the injected and withdrawn gas is set equal to the injectability or deliverability limit of that given hour. There are times when the actual injectability or deliverability of the reservoir cannot meet the demand placed by the dispatch. The reservoir pressure roughly follows the inventory level, while the wellhead pressure exhibits sharp changes, especially during 2010–2011. Tables 1 and 2 provide the net cash flow and emissions for the base case from 2010 to 2012. The average cash flow remains negative, as seen in Table 1, at about $1.5 million. In Table 2 it can be seen that project emits about 1290 t of $CO_2$ annually.

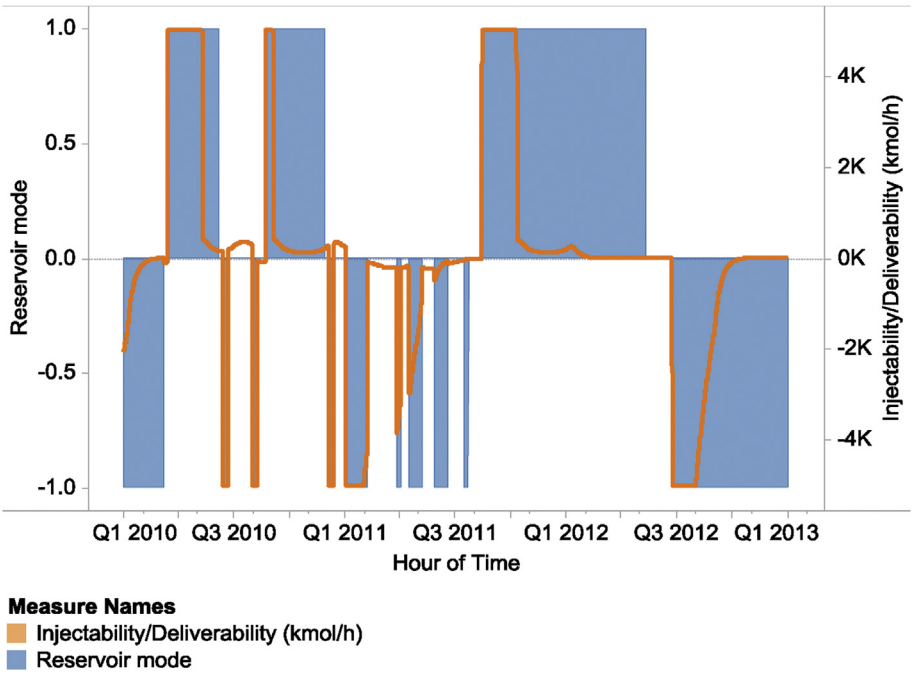


**Fig. 2.** Injectability/deliverability and dispatch to reservoir for the base case scenario.

**Table 1**
Net annual cash flow for the base case scenario.

| Annual cash flow | 2010 | 2011 | 2012 | Average |
|---|---|---|---|---|
| 1. Capital costs | $ (290,000) | $ (290,000) | $ (290,000) | $ (290,000) |
| 2. OM costs | $ (99,000) | $ (99,000) | $ (99,000) | $ (99,000) |
| 3. Cost of sales | $ (15,792,000) | $ (23,702,000) | $ (16,411,000) | $ (18,635,000) |
| 4. Sales | $ 14,881,000 | $ 21,533,000 | $ 16,274,000 | $ 17,563,000 |
| 5. Annual net | $ (1,300,000) | $ (2,559,000) | $ (526,000) | $(1,462,000) |

**Table 2**
Summary of environmental performance for the base case scenario.

| Environmental performance | 2010 | 2011 | 2012 | Average |
|---|---|---|---|---|
| **Emission incurred (kg $CO_2$/year)** | | | | |
| Compression of natural gas | 2.18E+06 | 1.67E+06 | 2.75E+04 | 1.29E+06 |
| Grid power generation for $H_2$ Mixture use at CCGT | | | | |
| Wind power generation for $H_2$ Off-site mixture use | 1.76E+08 | 2.81E+08 | 3.24E+08 | 2.60E+08 |
| **Emission mitigated (kg $CO_2$/year)** | | | | |
| Displacement of SMR $H_2$ Off-site NG use | 1.76E+08 | 2.81E+08 | 3.24E+08 | 2.60E+08 |
| NG use at CCGT | | | | |
| **Net emission calculation (kg $CO_2$/year)** | | | | 1.29E+06 |

### 3.2. Second scenario: hydrogen injection

In the second scenario, hydrogen is injected into the reservoir, along with the natural gas. The flow rates of hydrogen in and out of the reservoir are the same as the deliverability and injectability values set by the reservoir model, as shown in Fig. 3. The conditions in the reservoir are similar to those in the first scenario, except for the presence of hydrogen which averages 2% over the 3-year period. The concentration of the mixture stream injected into the reservoir varies widely, from negligible amounts up to 100%. High concentrations of hydrogen occur when the flow rate of natural gas is low, as shown by Fig. 4. Regardless of the high concentration of the stream, the reservoir concentration stays well below the 5% maximum.

In Tables 3 and 4, below, the net cash flow and the emissions for the second scenario are given.

### 3.3. Long term scenario: surplus base load generation reduction

In the third scenario, the energy hub produces hydrogen for energy storage and to deliver stored energy to the grid as electricity via CCGT. The dispatch issued to the reservoir is based on the deviation of Ontario's power demand from its annual moving average, as shown in Fig. 5. Spring and autumn are periods of injection, while summer and winter are periods of withdrawal. The inventory level for this scenario follows the seasonal pattern dictated by the dispatch orders, with peaks during spring and autumn and troughs during summer and winter. The 3-year average hydrogen

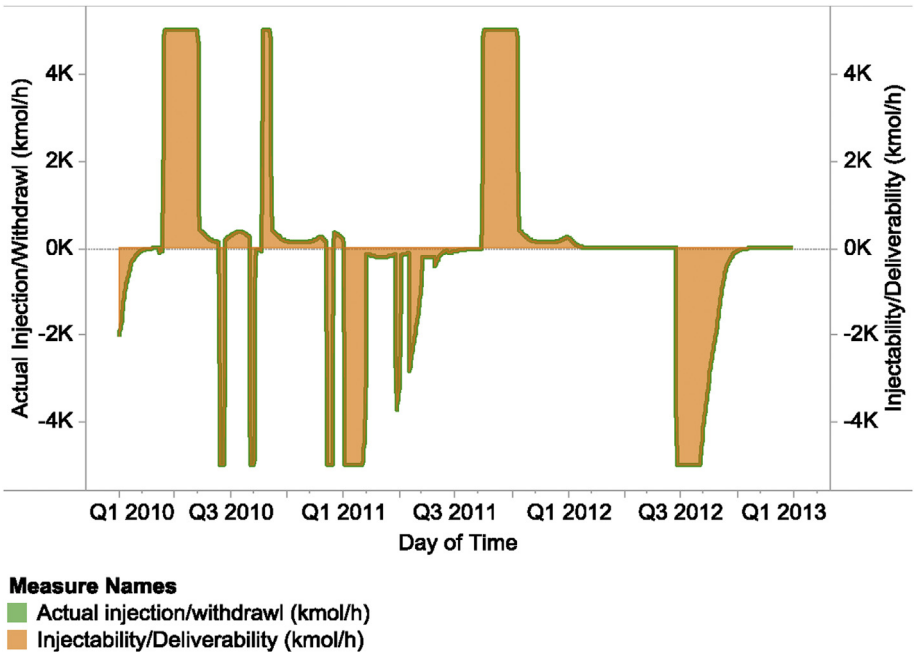


**Fig. 3.** Injectability/deliverability and actual reservoir flow rates for the hydrogen injection scenario.

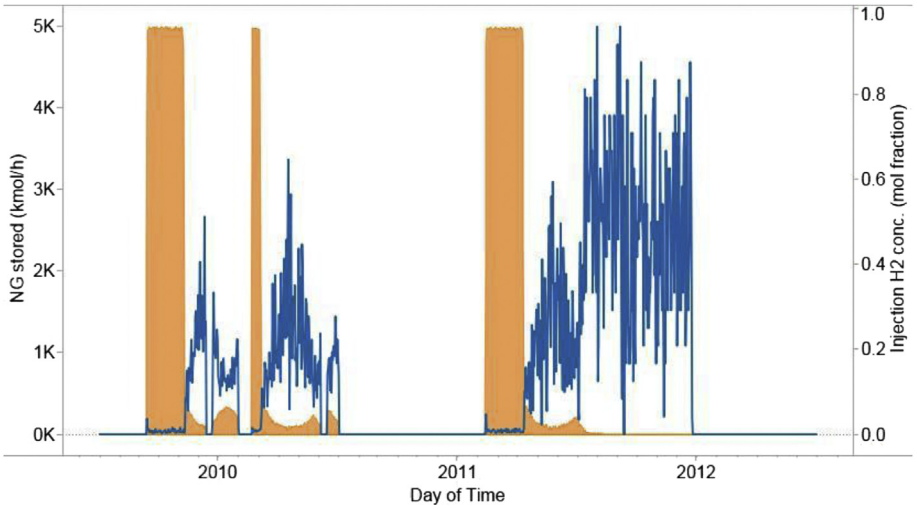


**Fig. 4.** Flow rates of injected streams for the second scenario.

**Table 3**
Net annual cash flow for the hydrogen injection scenario.

| Annual cash flow | 2010 | 2011 | 2012 | Average |
|---|---|---|---|---|
| 1. Capital costs | $ (2,979,000) | $ (2,979,000) | $ (2,979,000) | $ (2,979,000) |
| 2. OM costs | $ (236,000) | $ (236,000) | $ (236,000) | $ (236,000) |
| 3. Cost of sales | $ (16,198,000) | $ (22,337,000) | $ (22,544,0000) | $ (20,360,000) |
| 4. Sales | $ 15,935,000 | $ 23,056,000 | $ 19,245,000 | $ 19,412,000 |
| 5. Annual net | $ (3,478,000) | $ (2,496,000) | $ (6,515,000) | $(4,163,000) |
| **Difference from Base Case ($/year)** | | | | **$ (2,701,000)** |

concentration inside of the reservoir is 1%. The profile is relatively flat, except when hydrogen is introduced to the reservoir. As the trigger signal equals the difference from the annual moving average of the power demand, the wellhead pressure undergoes many high frequency low-magnitude changes.

With a rated capacity of 8.7 MW, the 30 electrolyzer modules operate nearly every hour during low energy demand, consuming about 8 MW demand. During high demand, this drops to 2–3 MW, or about 30%. Approximately 60% of the hydrogen is injected into the reservoir. The rest is absorbed by the local hydrogen demand at the time of production. During some hours, even though hydrogen is being produced, the reservoir, filled with HENG, can no longer accept more gas for storage. Compared to the hydrogen concentration in the injected mixture of the previous scenario, the

**Table 4**
Summary of environmental performance for the hydrogen injection scenario.

| Environmental performance | 2010 | 2011 | 2012 | Average |
|---|---|---|---|---|
| **Emission incurred (kg $CO_2$/year)** | | | | |
| Compression of natural gas | 2.55E+06 | 2.10E+06 | 5.81E+05 | 1.74E+06 |
| Grid power generation for H2 | 5.88E+06 | 3.90E+06 | 4.18E+06 | 4.66E+06 |
| Mixture use at CCGT | | | | |
| Wind power generation for H2 | | | | |
| Off-site mixture use | 1.73E+08 | 2.71E+08 | 3.14E+08 | 2.53E+08 |
| **Emission mitigated (kg CO2/year)** | | | | |
| Displacement of SMR H2 | 2.50E+06 | 4.43E+06 | 7.22E+06 | 4.72E+06 |
| Off-site NG use | 1.76E+08 | 2.78E+08 | 3.20E+08 | 2.58E+08 |
| NG use at CCGT | | | | |
| **Net emission calculation (kg $CO_2$/year)** | | | | −3.41E+06 |
| **Difference from base case (kg $CO_2$/year)** | | | | **−4.71E+06** |

As shown in Table 4, the net mitigation of annual $CO_2$ production is significantly greater than the savings from SMR to electrolysis, as previously discussed.

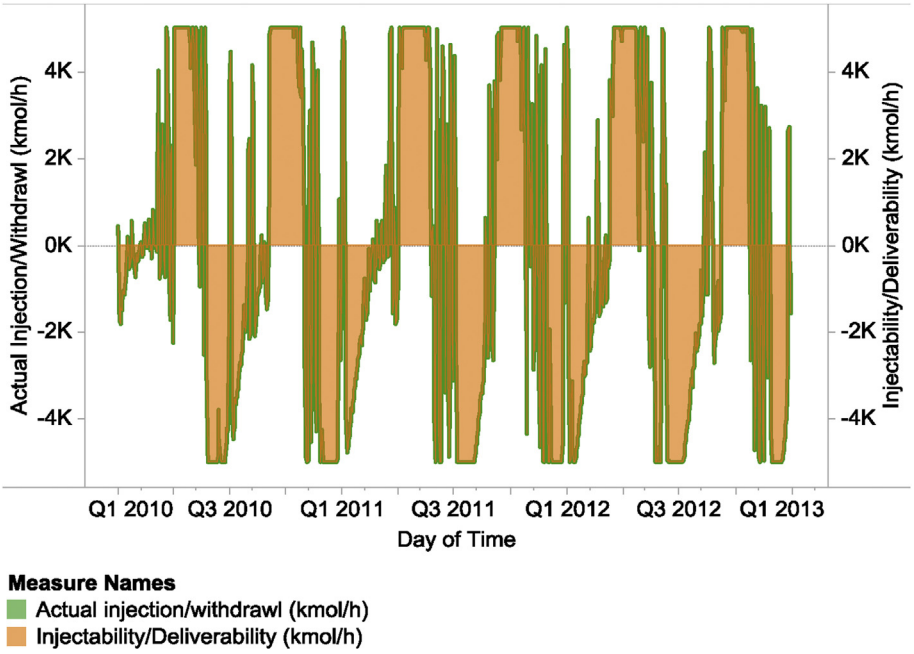


**Fig. 5.** Injectability/deliverability and actual reservoir flow rates for the surplus base load generation reduction scenario.

concentration in this scenario is much more stable, limited to the range of 0–30%. The average hydrogen concentration in the injected stream is 3%. As expected, the CCGT plant operates whenever there is a need to produce electricity from stored gas. The quantity of mixture consumed by the CCGT is less than 10% of that delivered to off-site customers. The average utilization of the CCGT is about 50%, which is the same as the electrolyzers. In Tables 5 and 6 the net cash flow and emission values for the third scenario are provided.

### 3.4. Long term scenario: integration of wind power

In the fourth scenario, components which allow for the storage and recovery of energy as hydrogen, and a small scale wind farm are part of the hub. The operation of the reservoir is optimized for use with wind power generation so that power generated off-peak is stored for delivery during peak periods. The injectability and deliverability curve of this scenario displays unique features, as shown in Fig. 6. Compared to the band of dense oscillating injections and withdrawals which last for most of the simulation, there is a singular increase during the first few months of storage operation. Further, the maximum deliverability below the axes in Fig. 6 is lower than the maximum injectability.

The reservoir is almost always full after it is filled, starting in 2010 and does not change cyclically. Although the inventory

**Table 5**
Net annual cash flow for the surplus base load generation reduction scenario.

| Annual cash flow | 2010 | 2011 | 2012 | Average |
|---|---|---|---|---|
| 1. Capital costs | $ (6,029,000) | $ (6,029,00) | $ (6,029,000) | $ (6,029,000) |
| 2. OM costs | $ (427,000) | $ (427,000) | $ (427,000) | $ (427, 000) |
| 3. Cost of sales | $ (46,981, 000) | $ (46,864, 000) | $ (37,270, 000) | $ (43,705, 000) |
| 4. Sales | $ 47,159, 000 | $ 48,057, 000 | $ 39,298, 000 | $ 44,838, 000 |
| 5. Annual net | $ (6,278, 000) | $ (5,263,000) | $ (4,430,000) | $ (5,323,000) |
| **Difference from Base Case ($/year)** | | | | **$ (3,862,000)** |

**Table 6**
Summary of environmental performance for the surplus base load generation reduction scenario.

| Environmental performance | 2010 | 2011 | 2012 | Average |
|---|---|---|---|---|
| **Emission incurred (kg $CO_2$/year)** | | | | |
| Compression of natural gas | 2.90E+06 | 3.29E+06 | 3.01E+06 | 3.07E+06 |
| Grid power generation for H2 | 4.07E+06 | 3.12E+06 | 2.87E+06 | 3.35E+06 |
| Mixture use at CCGT | 6.64E+07 | 6.55E+07 | 7.15E+07 | 6.78E+07 |
| Wind power generation for H2 | | | | |
| Off-site mixture use | 5.06E+08 | 5.89E+08 | 6.59E+08 | 5.85E+08 |
| **Indirect emission mitigated (kg $CO_2$/year)** | | | | |
| Displacement of SMR H2 | 2.70E+06 | 2.81E+06 | 3.13E+06 | 2.88E+06 |
| Off-site NG use | 5.12E+08 | 5.98E+08 | 6.68E+08 | 5.92E+08 |
| NG use at CCGT | 6.64E+07 | 6.55E+07 | 7.15E+07 | 6.78E+07 |
| **Net emission calculation (kg $CO_2$/year)** | | | | −4.04E+06 |
| **Difference from base case (kg $CO_2$/year)** | | | | **−5.34E+06** |

As can be seen in Table 6 above, the net annual emissions are equal to approximately −4000 t of $CO_2$, resulting in a reduction of about −5300 t over the base case.

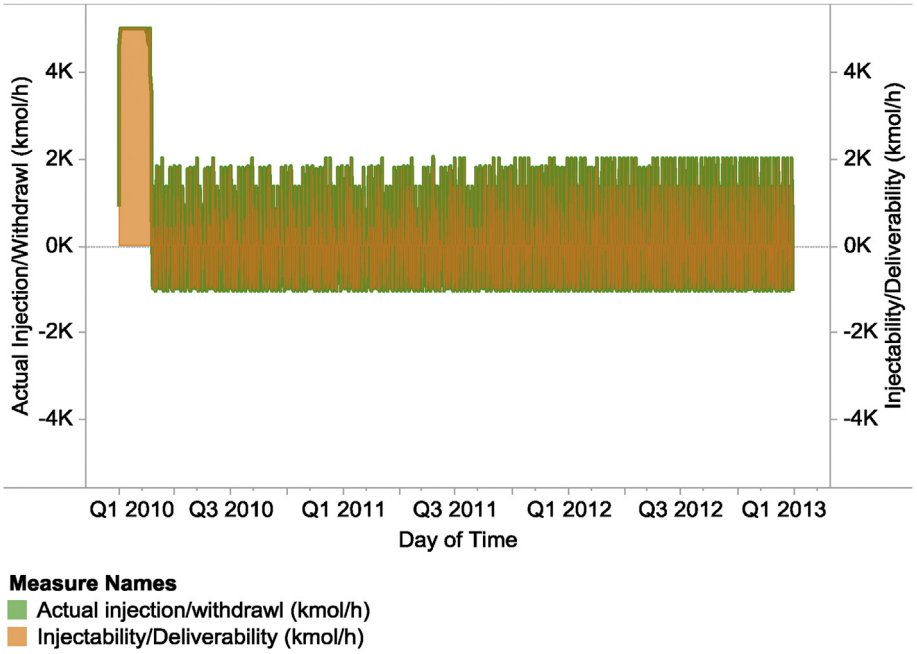


**Fig. 6.** Injectability/deliverability and actual reservoir flow rates for the wind power integration scenario.

remains consistent for much of the simulation, the concentration of hydrogen in the reservoir steadily climbs from 2% to 5%–6% yearly. The wellhead pressure changes within a very narrow range of pressures though it does not exhibit a trend. Observing the relationship between reservoir and wellhead pressures over the course of a month, it is observed that changes in wellhead pressure are frequent and small and rarely exceed the reservoir pressure. This can be attributed to the nature of changes in the trigger signal due to the duration and value of the feed-in tariff price for wind power.

The average capacity utilization factor of the wind turbines at the hub is approximately 25%. The capacity utilization factor of the electrolyzers is much higher than previous scenarios and experiences no yearly variation. Over 75% of the hydrogen produced by the electrolyzer is stored. Although the physical inventory of the reservoir remains its maximum capacity, the value of the gas stored in the reservoir is gradually decreasing. Note that the inventory value is computed based on the cost of inventory, not its marketable value. In Tables 7 and 8 the net cash flow and emissions for the current scenario are given. As can be seen in Table 7, the project has an average net cash flow of about -$11 million dollars, which is about $9 million dollars lower than in the base case. However, as shown in Table 8, the system provides about 4570t of $CO_2$ emissions reductions compared to the base case.

### 3.5. Long term scenario: meeting large hydrogen demand

In the fifth scenario, pure hydrogen is injected into a natural gas storage reservoir, with a pre-existing amount of natural gas present as a cushion gas. The signals on which reservoir operates are the schedule of hydrogen demand and the varying production of hydrogen which has a scale of 242 kmol/h. The actual flow rate of the injection is much smaller than the maximum injectability allowed by the reservoir conditions. At the same time, the flow rates withdrawn from the reservoir is largely limited by the deliverability, as shown in Fig. 7.

As in the fourth scenario, the inventory is nearly constant and devoid of the characteristics of storage cycles. However, the total inventory remains lower than in previous simulations. Due to the absence of natural gas injections, the concentration of hydrogen in the stored gas rises more rapidly than in the previous scenarios with annual average concentrations of 15%, 38% and 56%, for 2010–2012. Here, the wellhead pressure is volatile and does not

**Table 7**
Net annual cash flow for the wind power integration scenario.

| Annual cash flow | 2010 | 2011 | 2012 | Average |
|---|---|---|---|---|
| 1. Capital costs | $ (8,257,000) | $ (8,257,000) | $ (8,257,000) | $ (8,257,000) |
| 2. OM costs | $ (481,000) | $ (481,000) | $ (481,000) | $ (481,000) |
| 3. Cost of sales | $ (20,982,000) | $(21,742,000) | $ (18,751,000) | $ (20,492,000) |
| 4. Sales | $ 18,182,000 | $ 19,865,000 | $ 15,643,000 | $ 17,897,000 |
| 5. Annual net | $ (11,539,000) | $(10,616,000) | $ (11,847,000) | $ (11,334,000) |
| **Difference from base case ($/year)** | | | | **$ (9,873,000)** |

**Table 8**
Summary of environmental performance for the wind integration scenario.

| Environmental performance | 2010 | 2011 | 2012 | Average |
|---|---|---|---|---|
| **Emission incurred (kg $CO_2$/year)** | | | | |
| Compression of natural gas | 2.89E+06 | 1.76E+06 | 1.86E+06 | 2.17E+06 |
| Grid power generation for H2 | 7.07E+06 | 5.17E+06 | 5.18E+06 | 5.81E+06 |
| Mixture use at CCGT | 3.34E+07 | 3.89E+07 | 4.11E+07 | 3.78E+07 |
| Wind power generation for $H_2$ | 4.29E+05 | 4.20E+05 | 4.17E+05 | 4.22E+05 |
| Off-site mixture use | 1.70E+08 | 1.98E+08 | 2.09E+08 | 1.92E+08 |
| **Indirect emission mitigated (kg $CO_2$/year)** | | | | |
| Displacement of SMR $H_2$ | 2.36E+06 | 2.79E+06 | 2.99E+06 | 2.71E+06 |
| Off-site NG use | 1.74E+08 | 2.08E+08 | 2.22E+08 | 2.01E+08 |
| NG use at CCGT | 3.34E+07 | 3.89E+07 | 4.11E+07 | 3.78E+07 |
| **Net emission calculation (kg $CO_2$/year)** | | | | −3.28E+06 |
| **Difference from base case (kg $CO_2$/year)** | | | | **−4.57E+06** |

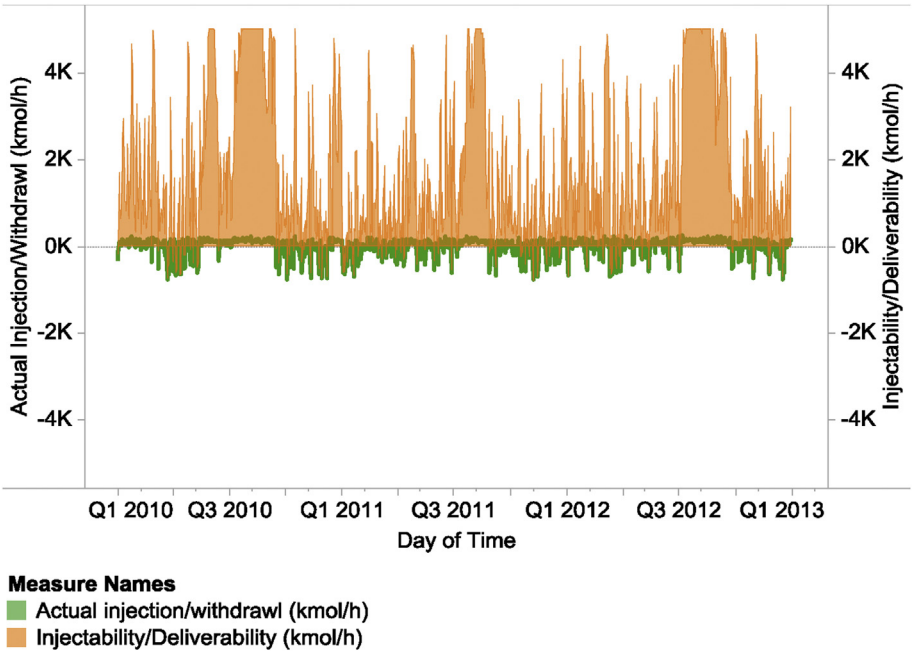


**Fig. 7.** Injectability/deliverability and actual reservoir flow rates for the large hydrogen demand scenario.

exhibit any clear trend.

The key factor differentiating this scenario from the others is the inflexibility of hydrogen demand. Previously, all of the hydrogen produced that cannot be stored is bought immediately. Once the hydrogen is produced, it can only be sold to a pre-scheduled customer. If there is no hydrogen demand, and the reservoir cannot accommodate the injection of hydrogen produced, then the amount of hydrogen in question is considered to be lost, or curtailed. Of all the hydrogen produced from the electrolyzer, 77% is stored, 10% is curtailed and 13% is delivered to pre-scheduled hydrogen demand.

The HENG produced from the reservoir is sent to the PSA to recovery pure hydrogen. The flowrate for the HENG is limited by the deliverability of the reservoir. The low injection and withdrawal flow rates lead to a somewhat static inventory, shown in Fig. 8. Unlike previous scenarios, in which the $H_2$ from the bypass is the only pure $H_2$, this scenario also allows pure hydrogen to be recovered using a PSA separator. The hourly flow rate of hydrogen that can be recovered through separation gradually increases, because the feed to the separator becomes richer in hydrogen with time. The separator is responsible for supplying approximately 73% of the hydrogen delivered to customers.

As illustrated in Fig. 8, the simulation manages to encapsulate the fluctuations in actual natural gas inventory levels. It is assumed

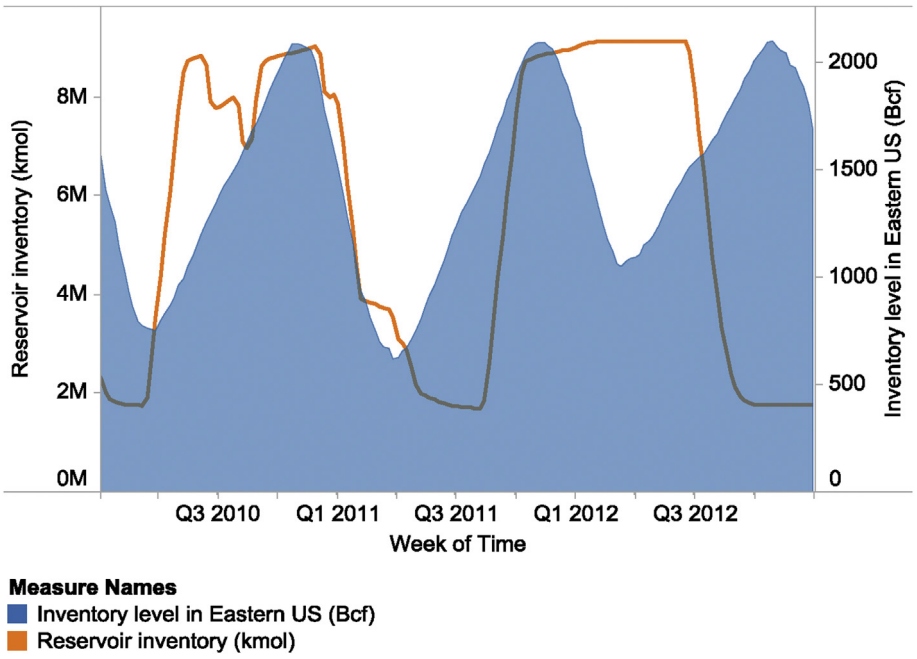


**Fig. 8.** Comparison of simulated and actual 2010–2012 inventory level for UGS facilities.

that the natural gas-rich adsorbate from the separator is marketed as HENG. The concentration of hydrogen in this stream has been lowered by undergoing the separation of hydrogen from natural gas in the PSA. When the reservoir concentration of $H_2$ reaches 60%, the concentration of the separator "effluent" is about 20%. The gas in the reservoir experiences a gradual decline in value over the course of three years. But this decline in value occurs at a much slower rate than the decrease in inventory value for the previous scenarios. In Table 9 and 10 the net cash flow and emission for the last scenario covered in this study is presented.

In Table 9, above, it can be seen that the average annual losses are about $8 million dollars which is about $3.8 million dollars less than the base case. In this scenario, however, the net emissions in Table 10 are positive at about 4400t annually, an increase of about 240% over the base case.

## 4. Discussion

Through the financial analysis it is found that the UGS facility at the heart of the UHNG technology, operated as specified in the reference scenario, leads to an average annual loss of over $1,400,000. This loss is caused by the imbalanced cost of sales and revenues shown in Fig. 9. The natural gas that is stored, on average, costs more than the price which it is sold at. Given that the sale of stored natural gas is the only source of revenue for the reference scenario, it is difficult to have a positive cash flow, as the revenue from natural gas sales are not enough to cover the cost of the stored gas.

**Table 9**
Net annual cash flow for the large hydrogen demand scenario.

| Annual cash flow | 2010 | 2011 | 2012 | Average |
|---|---|---|---|---|
| 1. Capital costs | $ (8,672,000) | $ (8,672,000) | $ (8,672,000) | $ (8,672,000) |
| 2. OM costs | $ (420,000) | $ - | $ - | $ (140,000) |
| 3. Cost of sales | $ (5,242,000) | $ (5,149,000) | $ (3,259,000) | $ (4,550,000) |
| 4. Sales | $ 4,530,000 | $ 6,230,000 | $ 5,506,000 | $ 5,422,000 |
| 5. Annual net | $ (9,803,000) | $ (7,591,000) | $ (6,425,000) | $ (7,940,000) |
| **Difference from base case ($/year)** | | | | **$ (3,777,000)** |

The cause of this cost imbalance is traced to the downward trend in the price of natural gas, during the simulation period, 2010–2012. The profitability of UGS operations is reliant upon the inter-seasonal difference in natural gas price, expected because of the seasonal changes in demand. But, as Fig. 10 shows, the seasonal term changes expected are suppressed by the larger market force depressing the price of natural gas over the course of several years, starting in late 2008.

The trend in the price of natural gas is a key factor influencing the operating profits of UGS facilities. The current approach involves determining project value based on average annual cash flow from a much shorter simulation period. This rests upon the underlying assumption that identical cash flow pattern can be expected for all future years of operation. This is an untenable position if the price of natural gas were to change significantly beyond the period of simulation. Therefore, when evaluating such a facility over its physical lifetime of over 20 years, it is preferable to forecast the long-term price of natural gas over the course of its lifetime, while extending the simulation to the expected lifetime of the project. For the same reason, the net present value of the energy hub is not calculated using the short-term average cash flows, because it is not representative of the long-term average annual cash flows which are used in net present value calculations. Compared to the reference scenario, the expected net cash flow of all future scenarios decreased further, as shown in Fig. 11. Here, all costs are shown as negative, so that the annual net cash flow is the sum of all five items. Besides the change in capital cost, the differences between the scenarios are mainly driven by the changes in the operating profits, the sales and cost of sales are further broken down to be compared.

### 4.1. Hydrogen injection

In the second scenario, the additional cost is mostly attributable to the capital cost requirement of the electrolyzer units. There is also a modest increase in operating profits of $124,515. However, this increase in profits, which is mostly from the sales of unstored

**Table 10**
Summary of environmental performance for the large hydrogen demand scenario.

| Environmental performance | 2010 | 2011 | 2012 | Average |
|---|---|---|---|---|
| **Emission incurred (kg $CO_2$/year)** | | | | |
| Compression of natural gas | 9.81E+05 | 1.18E+06 | 1.32E+06 | 1.16E+06 |
| Grid power generation for $H_2$ | 1.76E+07 | 1.17E+07 | 1.25E+07 | 1.40E+07 |
| Mixture use at CCGT | | | | |
| Wind power generation for $H_2$ | | | | |
| Off-site mixture use | 3.01E+07 | 2.45E+07 | 1.31E+07 | 2.26E+07 |
| **Indirect emission mitigated (kg $CO_2$/year)** | | | | |
| Displacement of SMR H2 | 5.03E+06 | 9.48E+06 | 1.03E+07 | 8.27E+06 |
| Off-site NG use | 3.12E+07 | 2.75E+07 | 1.64E+07 | 2.51E+07 |
| NG use at CCGT | | | | |
| **Net emission calculation (kg $CO_2$/year)** | | | | 4.38E+06 |
| **Difference from base case (kg $CO_2$/year)** | | | | **3.09E+06** |

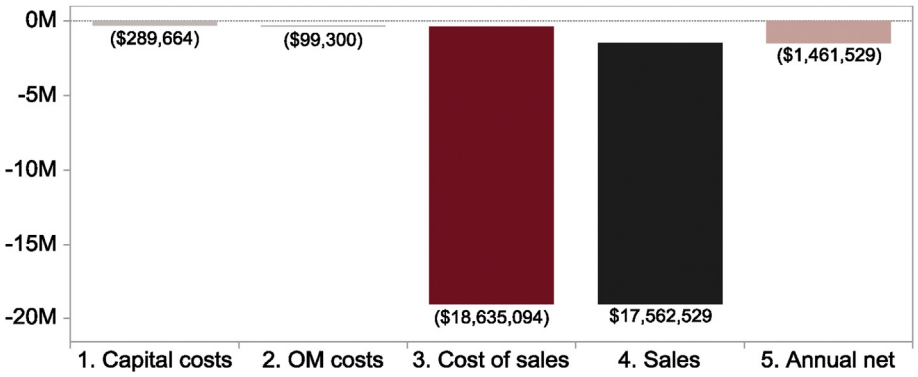


**Fig. 9.** Waterfall chart for the expected annual cash flow of the base case scenario.

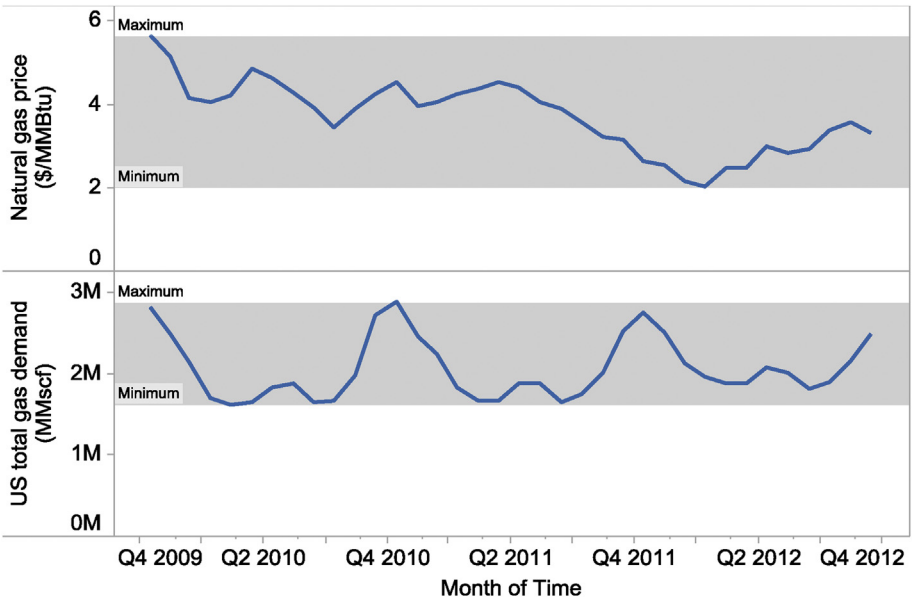


**Fig. 10.** Seasonal and annual trend in natural gas price and demand for 2010–2012.

hydrogen, but sold directly to meet local demand, barely covers the increased annual O&M costs. As the largest share of revenues is from the sales of HENG, the best course of action to increase revenues is to increase the price of HENG. Given that the average amount of the mixture delivered annually is $5.9 \times 10^6$ kmol and the average concentration of hydrogen in the reservoir is 2%, or 0.75 MMBtu/kmol, the annual output of mixture, in terms of energy is $4.4 \times 10^6$ MMBtu. Supposing everything else remains equal, the increase in price per energy delivered needs to be \$0.60/MMBtu or 16% of the 2010–2012 natural gas prices average of \$3.77/MMBtu to cover the additional capital costs.

If the price of HENG cannot be increased, another option to offset the cost of the electrolyzers is to increase the quantity of hydrogen directly delivered to meet local demand. However, not all of the unstored hydrogen can be absorbed by local demand.

In the third scenario, the sales and costs have increased

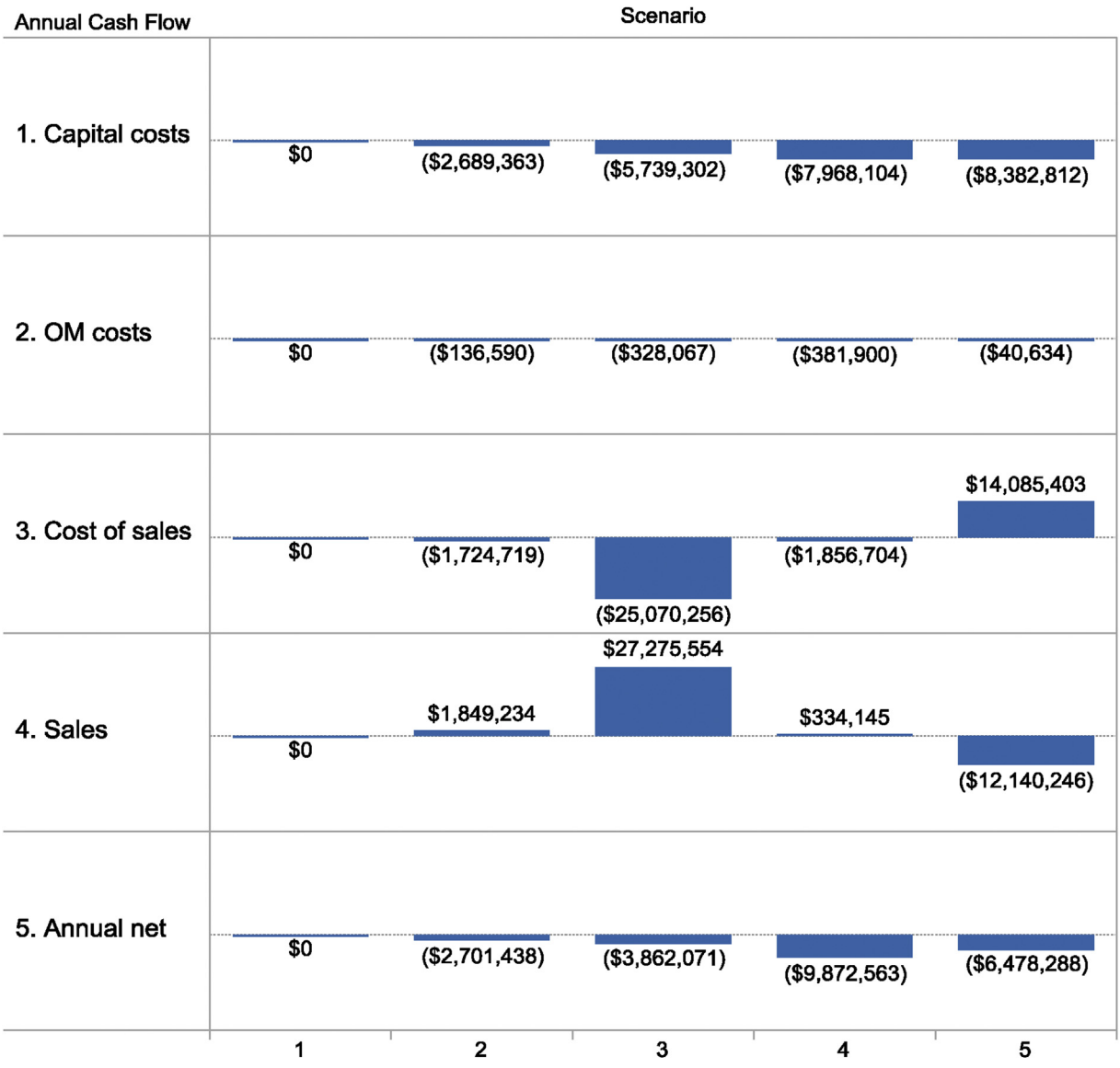


**Fig. 11.** Comparison of financial performance of all scenarios, all values are displayed relative to the base case value.

significantly. This change in throughput is caused by the change in the reservoir dispatch model logic at decision point D1, reducing the period of a storage cycle from 21 months to 6 months. This mirrors the peak and off-peak periods of power demand. The decrease in periods of storage cycles is also associated with a heightened throughput through the reservoir. Such a change can be realized practically only if the downstream gas distribution system can accommodate the increased throughput.

Furthermore, operating profit increases to $2,205,298, which partially offsets the additional capital cost of electrolyzers and CCGT. The sale of pure $H_2$ and power generated by the on-site CCGT contribute to this increased profit. It is believed that increasing the utilization factor of the electrolyzer and of the CCGT may further increase the operating profit. In this case, more of the capital cost will be offset, for the profit margin for hydrogen delivery and power delivery is higher than for HENG delivery. However, the capacity utilization factors are limited by the decision point logic specified for this scenario. The electrolyzers responsible for producing $H_2$ to charge the reservoir are only run when demand is low (D2), and the CCGT, which is responsible for discharging the reservoir by producing electricity, is only run when demand is high (D5). It is assumed that the reservoir cannot charge and discharge at the same time, therefore the utilization factor of each of those components cannot exceed 50%. Unless the revenues from the sales of HENG are increased, an operating loss is inevitable due to the capital cost of the electrolyzers and CCGT.

At its current scale of energy storage and release, the effect of the hub on short-term surplus base load generation is minimal. It is possible for the storage reservoir to accommodate all of the surplus energy available, shown in Fig. 12 as approximately 370,800 MWh for 10 days, as its rated storage capacity is 25,000 to 582,000 MWh. However, the majority of the surplus base load generation is available for short periods, with power ranging from hundreds to thousands of MW. The rate at which energy can be stored or delivered by the energy hub varies from 3 to 8 MW and 30–40 MW, respectively, due to the sizing of the electrolyzer technology being simulated. This range of power is much too low to absorb any sizeable portion of the surplus base load generation.

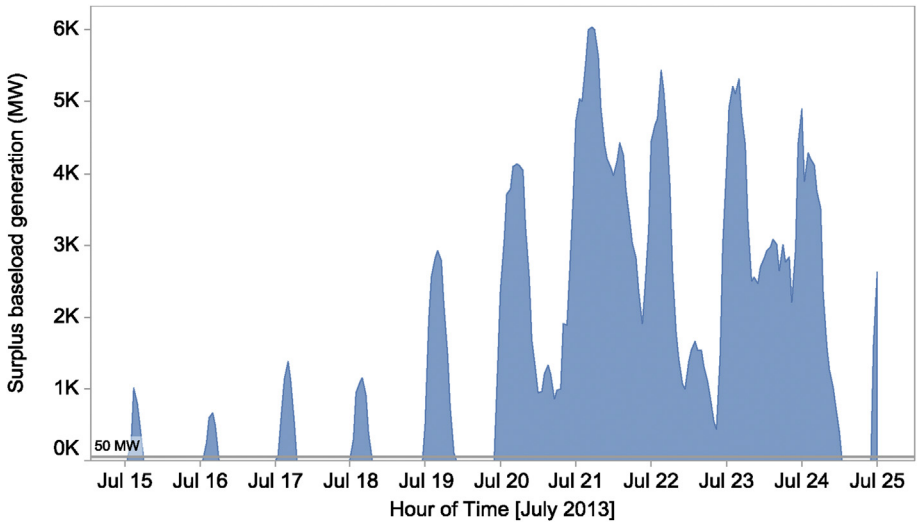


**Fig. 12.** Forecast surplus base load generation report for July 2013 from the IESO.

### 4.2. Wind power integration

In the fourth scenario, the operating profit decreases by $1,552,559, so that the annual loss is higher than the additional capital investment required. In Fig. 13, it is shown that although the cost of natural gas purchased from the gas grid increases, the sales of HENG to the grid decreases. This is likely caused by the increase in inventory level occurring in this scenario, which is caused by the short duration of the withdrawal window. The FIT schedule with time differentiation, as defined by the Ontario Power Authority, is used as the signal on which reservoir operations are based (D1) (OPA, 2015). Here, the 128 weekly off-peak hours, which incentivize energy storage, outnumber the 40 weekly peak hours, which encourage energy production.

As wind-turbines are included in the hub, the Fourth Scenario is capital-intensive. However, the inclusion of wind turbines does not improve the net cash flow of the energy hub. In terms of the operating profit, the direct sales of wind power is the most profitable when compared to all other options: recovering wind power as bypassed hydrogen, recovering wind power as power generated by the CCGT, or recovering wind power as energy contained in the hydrogen/natural gas mixture. In Table 11, the profit per unit of power generated by wind, natural gas or electricity is given. This illustrates the high value of wind power, due to the freely available wind, and the importance of following a particular energy stream.

Therefore, unless special consideration is given to these other pathways through pricing or incentives, there is no reason for the hub operator to store wind power during off-peak hours. Selling all wind power disregarding its time of production seems to be the most profitable use of wind turbines.

### 4.3. Large hydrogen demand

In Scenario 5, unlike in contrast with the 3rd scenario in which the volumes and cost of sales both increased, the two indicators decreased. This is due to the smaller scale of injection and withdrawal since only $H_2$ is injected and the mixture is only dispatched to the separator so that HENG can be recovered in its pure form. The resulting increase in operating profit is $1,945,157 and occurred mostly from the increased sales of pure hydrogen.

This increase, however, is not enough to offset the increase in capital cost required by the electrolyzers scaled up for this scenario. For this particular scenario, the rated capacity of the electrolyzer is increased which increases the capital cost significantly. On the other hand, the separator, although underutilized is only about 4% of the capital cost.

In three years, the concentration of hydrogen in the reservoir increases to 60%. If the operations are maintained, in 2–3 further years, the hydrogen concentration reaches levels above 90%. As the hydrogen concentration increases, the output of hydrogen by the separator also increases. It might be necessary to adjust the quantity of mixture withdrawn for separation if the hydrogen demand cannot accommodate this increase.

### 4.4. Effect of decision variables on environmental performance indicators

The emission profiles of the last four scenarios are compared to the reference case. The amount of emissions incurred by the energy hub and potential emissions mitigated varied widely from one scenario to another. However, their relative difference, the net emission, remained relatively constant for scenarios 2, 3, and 4: net reductions in emission in the order of 5000 tons per year are observed. Only scenario 5 deviates from this trend: a net increase in of 3000 tons per year is observed, as shown in Fig. 14.

The production and storage of hydrogen in the natural gas pipelines reduces potential $CO_2$ emissions for natural gas users. However, it is found that the storage and withdrawal of hydrogen from the reservoir causes a slight net increase in emissions due to the energy required in these tasks. Given the current power supply mix in Ontario, the amount of $CO_2$ indirectly emitted by grid-connected electrolyzers to produce hydrogen is far below the levels caused by producing hydrogen via steam methane reforming (SMR).

## 5. Conclusions

Within the scope of this study, the composite technology of Power-to-Gas and underground storage of hydrogen with natural gas (UHNG) is proposed and studied using a scenario-based modeling approach. A total of five scenarios are developed for this simulation study. Each of the scenarios targets a particular use of energy storage through UHNG, with the exception of the base

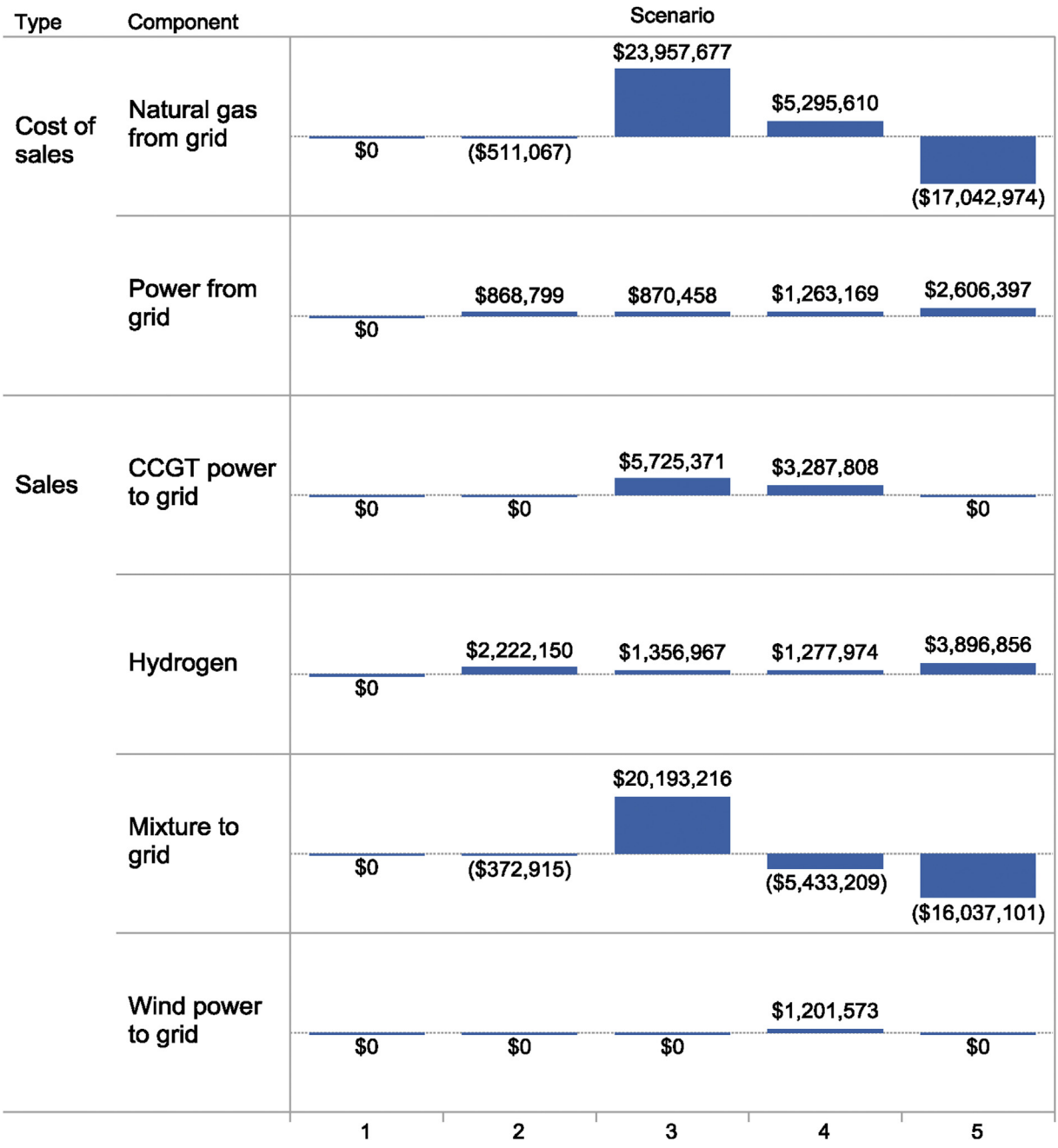


**Fig. 13.** Comparison of operating profits for all scenarios, all values are displayed relative to the base case value.

**Table 11**
Comparison of average profit per energy unit recovered for different storage pathways.

| Input | Value | Unit | $/unit | Conversion? | Eff. | Output | | Unit | $/unit | Profit per unit |
|---|---|---|---|---|---|---|---|---|---|---|
| Wind | 1 | MWh | 0 | NO | 100% | Wind | 1.00 | MWh | 115 | 115.00 |
| Wind | 1 | MWh | 0 | Electrolyzer | 70% | Bypassed H2 | 17.77 | kg H2 | 5 | 88.83 |
| Grid | 1 | MWh | 30 | Electrolyzer | 70% | Bypassed H2 | 17.77 | kg H2 | 5 | 58.83 |
| Grid | 1 | MWh | 30 | Elect. + separator | 56% | Separated H2 | 14.21 | kg H2 | 5 | 41.07 |
| Wind | 1 | MWh | 0 | Elect. + CCGT | 35% | CCGT | 0.35 | MWh | 30 | 10.50 |
| Wind | 1 | MWh | 0 | Electrolyzer | 70% | Mix | 2.39 | MMBtu | 3.7 | 8.84 |
| NG | 1 | MMBtu | 3.7 | CCGT | 50% | CCGT | 0.15 | MWh | 30 | 0.69 |
| NG | 1 | MMBtu | 3.7 | NO | 100% | Mix | 1.00 | MMBtu | 3.7 | 0.00 |
| Grid | 1 | MWh | 30 | Elect. + CCGT | 35% | CCGT | 0.35 | MWh | 30 | −19.50 |
| Grid | 1 | MWh | 30 | Electrolyzer | 70% | Mix | 2.39 | MMBtu | 3.7 | −21.16 |

Conversion factors: 1 MWh = 3.413 MMBtu, 1 MWh = 25.38 kg $H_2$ (based on HHV), 1 MMBtu = 0.29 MWh

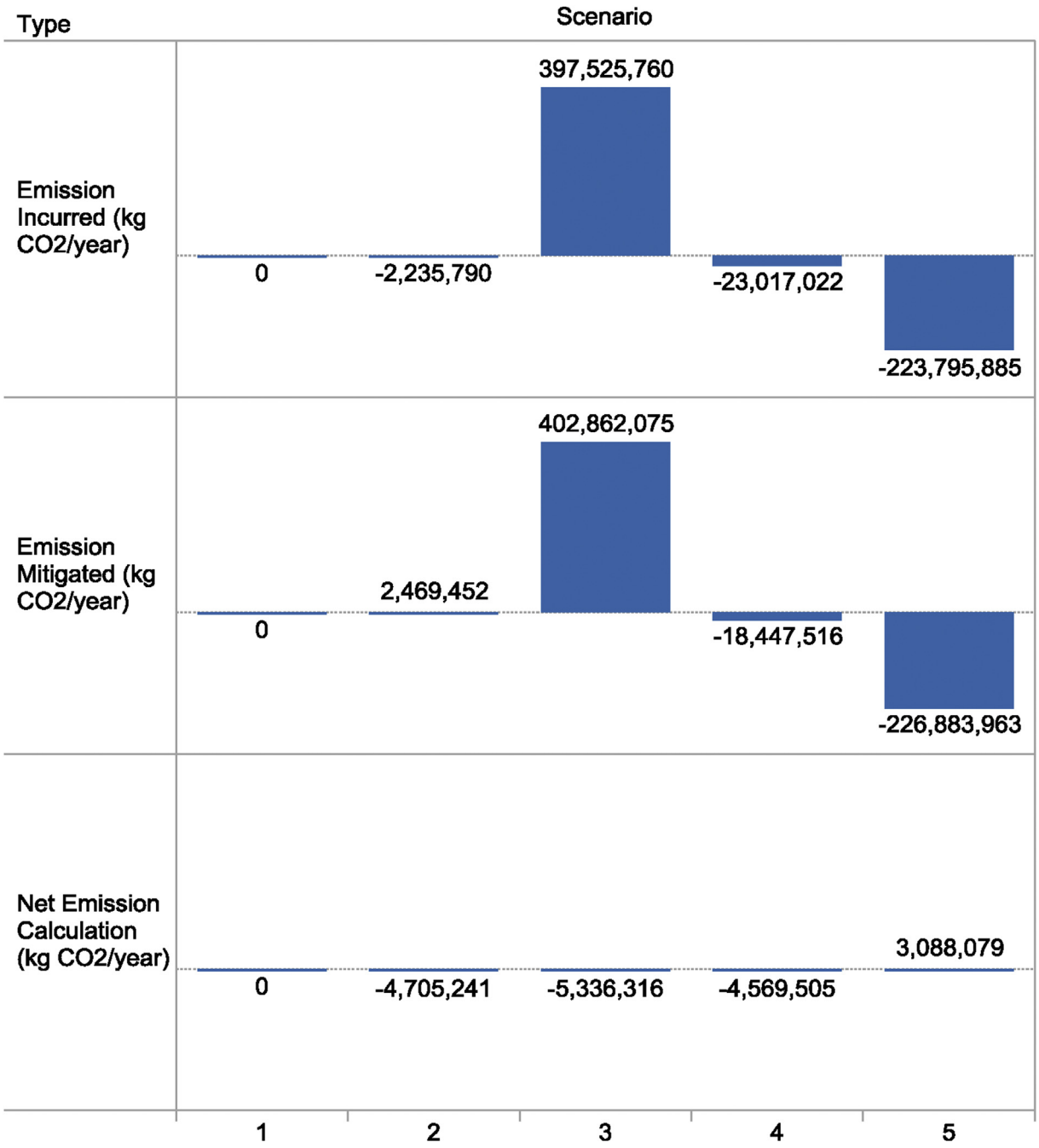


**Fig. 14.** Comparison of environmental performance of all scenarios, all values are displayed relative to the base case value.

case scenario, in which a basic underground gas storage facility is simulated, without on-site production and storage of hydrogen. All of the scenarios are subjected to the same external factors, but the design and operating philosophy of the hub is altered for each case. The selection of a rated capacity for the energy hub components is based on the likelihood of investment, as they are sized to be smaller than the maximum allowable size. Of all five scenarios, the reference scenario, which only involves basic underground gas storage operations, is the only one which can be fully compared against actual data for model validation. It is found that existing natural gas storage practices are driven more by variations in the demand for natural gas than by the price of natural gas. If the hub operates using the decision point logic specified by the reference scenario, the energy hub incurs financial losses for the simulation period. The most desirable pathway for energy recovery and revenue for the 2nd scenario, where hydrogen is injected into the reservoir along with natural gas, is the distribution and use of hydrogen enriched natural gas (HENG) by off-site users. It is found that, if operated as the decision points have specified, at the end of three years, the concentration of hydrogen in the reservoir is expected to increase to 2%. It is not profitable to sell HENG at the same price as natural gas and thus, to cover the cost of electrolyzers, a 16% premium is needed for the mixture, based on the 2010–2012 average natural gas price of $3.7/MMBtu. The results for the 3rd scenario, which is aimed at reducing surplus base load generation, is set up using the difference between the hourly Ontario demand

and the annual average demand as a proxy signal. The estimated level of surplus base load generation shows both short-term and long-term variation. Due to the limited rated input/output of the energy hub compared to its capacity, it is preferable to target long-term trend in surplus base load generation instead of the hourly variations. If hydrogen is stored together with natural gas, then operating the energy hub to store/discharge long-term surplus base load generation will alter the pattern of natural gas flow into and out of the storage reservoir, increasing the throughput of gas through the reservoir and the frequency of storage cycles.

In the fourth scenario wind power is used and, the level of stored gas is somewhat constant throughout the simulation. The scenario is not financially sustainable as the energy recovered from wind power in the form of hydrogen, mixed gas or electricity is not recognized and given a price different from the market value. With the current prices of electricity and natural gas, not enough can be made to pay for the increase in infrastructure. In the fifth scenario, where only $H_2$ is stored inside the reservoir with the intention of meeting a large future hydrogen demand scenario, if the energy hub is operated as the scenario specifies, the concentration of $H_2$ inside the reservoir will increase to 60% after three years of storage. The current signals used to indicate a need for the storage or withdrawal of hydrogen are the time differentiated feed in tariff schedule and hydrogen pick-up schedule centered around working hours. As both of these signals are unbalanced, having more off-peak hours than peak hours, indicating that the storage reservoir is more often charged than discharged.

Overall, compared to the reference scenario, the other four scenarios all incurred annual losses. In terms of emissions, scenario 2, 3, and 4 had little effect on emission. In scenario 5, however, much greater emissions reductions were realized due to the larger scale for production and storage of $H_2$. In future, the commodity price of hydrogen, as well as the potential earnings through selling carbon credits, will be considered.

## Acknowledgment

This paper was written with the support of National Science and Engineering Research Council and Ontario Center of Excellence, as well as our research partners Enbridge, Hydrogenics, Union Gas, GE, and Energy Technology & Innovation Canada (ETIC).

## Nomenclature

| Symbol | Physical constant | Units | Reference |
|---|---|---|---|
| $B_g$ | Gas formation volume factor | Unitless | Ikoku (1980) |
| $V_{max,\ s}$ | Maximum reservoir capacity for natural gas at standard volume | $m^3$ | Ikoku (1980) |
| $p_s$ | Standard pressure | Atm | Ikoku (1980) |
| $p_{res,max}$ | Maximum reservoir pressure | Atm | Ikoku (1980) |
| $p_{res,min}$ | Minimum reservoir pressure | Atm | Ikoku (1980) |
| $T_s$ | Standard temperature | K | Ikoku (1980) |
| $T_{res}$ | Reservoir temperature | K | Ikoku (1980) |
| $z_s$ | Standard compressibility factor | Unitless | Ikoku (1980) |
| $z_{res,max}$ | Maximum reservoir compressibility factor | Unitless | Ikoku (1980) |
| $P_{w,i}$; $P_{w,rated}$ | Rated capacity of turbine $i$ | MW | Vestas (2015) |
| $\alpha$ | Hellman exponent | Unitless | Kaltschmitt et al. (2007) |
| $E_{HHV}$ | High heating value of hydrogen | MJ | NIST, 2015 |
| $MW_{H2}$ | Molar mass of hydrogen | G | NIST, 2015 |
| $HOEP(t)$ | Hourly Ontario Energy Price at time $t$ | $ | IESO, 2013 |
| $E_{NG}$ | Energy created by a unit of natural gas | MJ | NIST, 2015 |

| Symbol | Variable | Units |
|---|---|---|
| $V_{max}$ | Maximum reservoir pore volume | $m^3$ |
| $n_{tot}$ | Total gas at end of time step | Kg |
| $n_{tot,0}$ | Total gas at start of time step | Kg |
| $\dot{n}_{in}$ | Rate of gas in during time step | kg per h |
| $\dot{n}_{out}$ | Rate of gas out during time step | kg per h |
| $P_{res}$ | Average reservoir pressure | atm |
| $u_{80}$ | Wind speed 80 m above the ground | m per s |
| $u_{10}$ | Wind speed 10 m above the ground | m per s |
| $N_T$ | Number of turbines | Unitless |
| $\dot{n}_{E,H2,i}$ | Rate of $H_2$ production by electrolyzer $i$ | kg per h |
| $E_E$ | Overall energy requirement of the electrolyzer | MJ |
| $E_{E,s}$ | Stack energy requirement of the electrolyzer | MJ |
| $E_{E,o}$ | Other energy requirement of the electrolyzer | MJ |
| $\eta_{E,s}$ | Efficiency of the stacks of the electrolyzer | Unitless |
| $\eta_{CC}$ | Efficiency of the combined cycle gas turbine | Unitless |
| $\dot{w}_{GT}$ | Work generated by gas turbine | Nm |
| $\dot{w}_{ST}$ | Work generated by steam turbine | Nm |
| $\dot{H}_{GT}$ | Work inputted to gas turbine | Nm |
| $\dot{H}_{ST}$ | Work inputted to steam turbine | Nm |
| $\eta_{sep}$ | Efficiency of the separator | Unitless |
| $\dot{n}_{H2,sep}$ | Rate of hydrogen output from separator | kg per h |
| $\dot{n}_{H2,feed}$ | Rate of hydrogen fed to separator | kg per h |
| $C_{H2,\ feed}$ | Concentration of hydrogen in the feed stream | kg per $m^3$ |
| $C_{H2,\ prod}$ | Concentration of hydrogen in the product stream | kg per $m^3$ |
| $\dot{n}_{feed}$ | Rate of material fed to separator | kg per h |
| $\dot{n}_{prod}$ | Rate of material output from separator | kg per h |
| $W_{comp,\ th}$ | Isentropic work of compressor | Nm |
| $P_{comp}$ | Power required by compressor | Nm |
| $\dot{n}_{comp}$ | Rate of compressor gas flow material | kg per h |
| $\eta_{sep}$ | Isentropic compressor efficiency | Unitless |
| $\bar{z}$ | Average compressibility factor | Unitless |
| $k_{mix}$ | Heat capacity ratio of the compressed gases | Unitless |
| $S_{wtg}(t)$ | Sales of wind energy to the grid at time $t$ | MJ |
| $P_{wtg}(t)$ | Wind energy sold to the grid at time $t$ | MJ |
| $FIT(t)$ | Ontario time-of-day, or FIT, energy price at time $t$ | $ per MW |
| $S_{H2}(t)$ | Sales of hydrogen at time $t$ | Unitless |
| $C_{H2}(t)$ | Price of hydrogen at time $t$ | $ per kg |
| $S_{CCGTtG}(t)$ | Sales of combined cycle gas turbine energy to the grid | MJ |
| $W_{cc}(t)$ | Amount of energy produced by CCGT at time $t$ | MJ |
| $S_{mix}(t)$ | Sales of hydrogen enriched natural gas at time $t$ | MJ |
| $\eta_{mix}(t)$ | Molar flow rate of HENG at time $t$ | mol per h |
| $C_{mix}(t)$ | Cost of HENG at time $t$ | $ per kg |
| $E_{mix}(t)$ | Energy produced by HENG at a given time $t$ | MJ |
| $C_{Gts}(t)$ | Cost of power to the system at time $t$ | $ per MW |
| $C_{NGts}(t)$ | Cost of natural gas to the system at time $t$ | $ per kg |
| $P_{Gts}(t)$ | Amount of power taken from the grid to the system at time $t$ | MW |
| $\eta_{NGts}(t)$ | Amount of natural gas purchased at time $t$ | Kg |
| $C_{NG}(t)$ | Cost of natural gas at time $t$ | $ per kg |
| $C_{incurred}$ | Incurred cost of energy | $ per MJ |
| $C_{annual}$ | Annual cost of energy | $ per MJ |
| $I$ | Inventoried cost of purchases | $ |
| $I_i$ | Inventoried cost of purchase in year $i$ | $ |
| $I_{i,o}$ | Inventoried cost of purchase at the start of year $i$ | $ |
| $I_{i,f}$ | Inventoried cost of purchase at the end of year $i$ | $ |
| $C_{res,tot}(t)$ | Cost of gas in storage at time $t$ | $ |
| $C_{mix,\ unit,\ t}$ | Unit cost of mixed fuel stored at time $t$ | $ per kg |
| $\eta_{tot,\ t}$ | Total gas stored at time $t$ | Kg |
| $C_{inv,tot}$ | Total capital cost of the energy hub | $ |
| $C_{W,inv}$ | Total capital cost of wind turbines | $ |
| $C_{E,inv}$ | Total capital cost of electrolyzers | $ |
| $C_{sep,inv}$ | Total capital cost of seperators | $ |
| $C_{comp,inv}$ | Total capital cost of compressors | $ |
| $C_{CCGT,inv}$ | Total capital cost of combined cycle gas turbines | $ |
| $\dot{n}_{s,act}$ | Flowrate through the reservoir | kg per h |
| $\dot{n}_{H_2,S}$ | Amount of hydrogen that is stored | Kg |
| $\dot{n}_{H_2,E}$ | Amount of electrolytic hydrogen produced | Kg |
| $CEPCI_i$ | Chemical Engineering Plant Cost Index for year $i$ | Unitless |
| $\dot{n}_{H_2,E,rated,i}$ | Rated electrolytic hydrogen production by electrolyzer $i$ | kg per h |
| $P_{E,j}$ | Rated capacity of electrolyzer $j$ | MW |
| $N_E$ | Number of electrolyzers procured | Unitless |

(continued on next page)

(*continued*)

| Symbol | Variable | Units |
|---|---|---|
| $C_{E,inv,i}$ | Cost of electrolyzer *i* | $ |
| $C_{sep,ads}$ | Cost of adsorption beds | $ |
| $C_{sep,col}$ | Cost of PSA columns | $ |
| $C_{comp}$ | Cost of compressor | $ |
| $C_{OM,fixed}$ | Fixed cost of operations and maintenance | $ |
| $C_{OM,annual}$ | Annual cost of operations and maintenance | $ per year |
| $R_{OM}$ | Percentage of the fixed annual costs towards maintenance | Unitless |
| $NG_{COMP,NG}$ | Energy used to compress HENG, converted to natural gas | MJ |
| $P_{comp}$ | Power requirement of compressor | MW |
| *GPR* | Gas per unit of energy | kg per MJ |
| $E_{NG}$ | Energy content of natural gas | MJ per kg |
| $C_{comp,E}$ | Energy cost for running a compressor | MJ |
| $m_{CO_2,incurred}$ | Emissions incurred by the energy hub | kg $CO_2$e |
| $m_{CO_2,mitigated}$ | Emissions mitigated by the energy hub | kg $CO_2$e |
| $m_{CO_2,net}$ | Net emissions of the energy hub | kg $CO_2$e |
| $m_{CO_2,comp}$ | Emissions of the compressor | kg $CO_2$e |
| $m_{CO_2,G}$ | Emissions of the grid | kg $CO_2$e |
| $m_{CO_2,W}$ | Emissions produced by the wind farm | kg $CO_2$e |
| $m_{CO_2,CCGT}$ | Emissions from the combined cycle gas turbine | kg $CO_2$e |
| $m_{CO_2,mix}$ | Emissions produced from the HENG | kg $CO_2$e |
| $m_{CO_2,SMR}$ | Estimated emissions to produce hydrogen by steam methane reformation | kg $CO_2$e |
| $m_{CO_2,fuel}$ | Estimated emissions of burning fuel for energy | kg $CO_2$e |
| $m_{CO_2,NG}$ | Estimated emissions of natural gas | kg $CO_2$e |
| *Pcomp,rated* | Rated power of the compressor | MW |
| $W_{cc,rated}$ | Rated output of the combined cycle turbine | MW |

## Appendix 1. Sales revenues

The financial model used to estimate the profits of the system includes all possible sales, operating expenses and annualized fixed costs of the hub. The value of the hourly energy sales is determined by multiplying the hourly flow rate of the material or energy vector with the corresponding market price in place for the hour in question.

$$S_{wtG}(t) = P_{WtG}(t)FIT(t) \tag{20}$$

$$S_{H_2}(t) = \left[\dot{n}_{H_2,sep}(t) + \dot{n}_{H_2,b}(t)\right]MW_{H_2}C_{H_2} \tag{21}$$

$$S_{CCGTtG}(t) = \dot{W}_{CC}(t)HOEP(t) \tag{22}$$

$$S_{mix}(t) = \dot{n}_{mix,tot}E_{mix}(t)C_{mix}(t) \tag{23}$$

where $S_{WtG}$ is the sales of wind power to the grid at a given time t, $S_{H_2}$ is the sales of hydrogen to costumers, $S_{CCGTtG}$ is the sales of CCGT generated power to the grid at a given time t and $S_{mix}$ is the sales of hydrogen-enriched natural gas mixture to customers. $P_{wtG}(t)$ is the amount of power sold from the wind farm to the grid at time t and FIT(t) is the price for energy given by the FIT program in Ontario at time t (Ontario Power Authority, 2015).

## Appendix 2. Inventory

The value of *I* is positive if there is a net gain in the value of inventory compared to the beginning of the year or negative if there is a net loss. To determine the inventoried cost of purchase the value of the material in storage at the beginning and end of each year is needed.

$$I_i = \frac{I_{i,f} - I_{i,0}}{\Delta t} \tag{29}$$

$$I_{2010,0} = C_{res,tot}(t_0) \tag{30}$$

$$I_{2010,f} = I_{2011,0} = C_{res,tot}(t_1) \tag{31}$$

$$I_{2011,f} = I_{2012,0} = C_{res,tot}(t_2) \tag{32}$$

$$I_{2012,f} = C_{res,tot}(t_3) \tag{33}$$

where $I_i$ is the inventory cost of purchase of year i, $I_{i,f}$ and $I_{i,0}$ are the cost of inventory at the end and the beginning of year i and $C_{res,tot}$ is the cost of gas in storage at time t.

## References


Altfield, K., Pinchbeck, D., 2013. Admissable Hydrogen Concentrations in Natural Gas Pipelines. Reprint: gas for energy 03/2013 ISSN 2192–158X DIV Deutscher Industrieverlag GmbH. 2013. Retrieved February 10, 2015 from. http://www.gerg.eu/public/uploads/files/publications/GERGpapers/SD_gfe_03_13_Report_Altfeld-Pinchbeck.pdf.

Bachu, S., Dusseault, M.B., 2005. Underground injection of carbon dioxide in salt beds. Cavern Constr. Behav. 639–650.

Bajohr, S., Goetz, M., Graf, F., Ortlaff, F., 2011. Speicherung von regenerativ erzeugter elektrischer Energi in der Erdgasinfrastruktur. gwf-ErdGas 200–209.

Baxter, R., 2006. Energy Storage: a Nontechnical Guide. PennWell Books.

Brown, R.N., 1997. Compressors: Selection and Sizing. Elsevier Gulf.

Bunger, U., 2014. Overview and tentative results of the HyUnder project, 2014. In: Presented at Joint NOW GmbH – FCH JU Water Electrolysis Day, 3 April 2014, White Atrium, Avenue de la Toison d'Or 56-60, 1060 Brussels, Belgium.

Chung, Y., Na, B., Song, H., 1998. Short-cut evaluation of pressure swing adsorption systems. Comput. Chem. Eng. 22, S637–S640.

Clarke, J., 2012. In: Dan Peng (Ed.), Correspondence with Senior Geologist from Union Gas.

Crotogino, F., Donadei, S., Bunger, U., Landinger, H., 2010. Large-scale underground storage for securing future energy supplies. In: Proceedings of the World Hydrogen Energy Conference 2010, May 16-21, 2010, pp. 36–46. Essen. 78.4.

Dranchuk, P.M., Purvis, R.A., Robinson, D.B., 1973, January. Computer calculation of natural gas compressibility factors using the Standing and Katz correlation. In: Annual Technical Meeting. Petroleum Society of Canada.

Dusseault, M.B., Bach, S., Rothenburg, L., 2004. Sequestration of $CO_2$ in salt caverns. J. Can. Petroleum Technol. 43.11, 49–55.

Electric Power Research Institute, 2010. Electricity Energy Storage Technology Options. CA. White Paper, Palo Alto.

Elsharkawy, A.M., Elkamel, A., 2001. The accuracy of predicting compressibility factor for sour natural gases. Petroleum Sci. Technol. 19 (5–6), 711–731.

European Union, 2015. Final Report Summary - HYUNDER (Assessment of the Potential, the Actors and the Relevant Business Cases for Large Scale and Seasonal Storage of Renewable Electricity by Hydrogen Underground Storage in Europe). Technical report, project 303417.

Fatoorehchi, H., Abolghasemi, H., Rach, R., 2014. An accurate explicit form of the Hankinson–Thomas–Phillips correlation for prediction of the natural gas compressibility factor. J. Petroleum Sci. Eng. 117, 46–53.

Fatoorehchi, H., Abolghasemi, H., Rach, R., Assar, M., 2014a. An improved algorithm for calculation of the natural gas compressibility factor via the Hall-Yarborough equation of state. Can. J. Chem. Eng. 92 (12), 2211–2217.

Foh, S., Novil, M., Rockar, E., Randolph, P., 1979. Underground Hydrogen Storage Final Report. Institute of Gas Technology, Chicago.

Germany Trade & Invest, 2012. Green Hydrogen and Power-to-Gas Technology Mass Energy Storage for the Future Energy Market. Fact Sheet.

IESO, 2013. Forecast Weekly Minimum Demand and Base Load Generation, 2013, 18MonthOutlookTables_2013may.

IESO, 2015. IESO Power Data 2015. Retrieved from. May 19, 2015. http://www.ieso.ca/Pages/Power-Data/default.aspx.

Ikoku, C.U., 1980. PennWell Books, Tulsa, p. 788. Natural Gas Engineering: A system Approach.

International Renewable Energy Agency, 2012. Wind power. In: Renewable Energy Technologies: Cost Analysis Series. International Renewable Energy Agency.

Kaltschmitt, M., Striecher, W., Weise, A., 2007. Renewable Energy: Technology, Economics and Environment. Springer, New York.

Mannan, P., Baden, G., Olein, L., Bradon, C., Scorfield, B., Naini, N., Cheng, J., 2014. Techno-economics of Energy Storage. Technical Report. Alberta Innovates – Technology Futures and BECL and Associates Ltd.

Melaina, M.W., Antonia, O., Penev, M., 2013. Blending Hydrogen into Natural Gas Pipeline Networks: a Review of Key Issues. National Renewable Energy Laboratory. Technical Report: NREL/TP-5600–51995.

National Energy Storage Technology, 2010. Cost and Performance Baseline for Fossil Energy Plants Volume 1: Bituminous Coal and Natural Gas to Electricity Revision 2 2010. Technical Report DOE/NETL-2010/1397.

NIST Chemistry Webbook, 2015. National Institute of Standards and Technology. Retrieved from: http://webbook.nist.gov/chemistry/on February 12th, 2015.

Ontario Ministry of Energy, 2012. Ontario's Feed-in Tariff Program Two-year Review Report. Ontario Ministry of Energy, Toronto.

Ontario Power Authority, 2015. FIT Price Schedule. Retrieved from. on March 23, 2015. http://fit.powerauthority.on.ca/fit-program/fit-program-pricing/fit-price-schedule.

Peng, D., 2013. Enabling Utility-scale Electrical Energy Storage through Underground Hydrogen-natural Gas Co-storage. Master of Applied Science in Chemical Engineering. University of Waterloo.

Sandia National Research Laboratories, 2013. DOE/EPRI 2013 Electricity Storage Handbook in Collaboration with NCREA. Report, July 2013.

Schouten, J.A., Janssen-van Rosmalen, R., Michels, J.P.J., 2006. Modeling hydrogen production for injection into the natural gas grid: balance between production, demand and storage. Int. J. Hydrogen Energy 31.12, 1698–1706.

Schouten, J.A., Michels, J.P.J., Janssen-van Rosmalen, R., 2004. Effect of H2-injection on the thermodynamic and transportation properties of natural gas. Int. J. Hydrogen Energy 29, 1173–1180.

Stone, H.B.J., Veldhuis, I., Richardson, R.N., 2009. Underground hydrogen storage in the UK. In: Evans, D.J., Chardwin, R.A. (Eds.), Underground Gas Storage: Worldwide Experiences and Future Development in the UK and Europe. The Geological Society, London, pp. 217–226.

Venter, R.D., Pucher, G., 1997. Modelling of stationary bulk hydrogen storage systems. Int. J. Hydrogen Energy 22.8, 791–798.

Vestas, 2015. V90–2.0MW Technical Specifications. Retrieved 2015-02-15 from. http://www.vestas.com/en/products_and_services/turbines/v90-2_0_mw#!technical-specifications.